NASA Contractor Report 4142

Nonlinear Wave Interactions in Swept Wing Flows

Nabil M. El-Hady

GRANT NAG1-729
MAY 1988

NASA

NASA Contractor Report 4142

Nonlinear Wave Interactions in Swept Wing Flows

Nabil M. El-Hady
Old Dominion University
Norfolk, Virginia

Prepared for
Langley Research Center
under Grant NAG1-729

National Aeronautics
and Space Administration

**Scientific and Technical
Information Division**

1988

NONLINEAR WAVE INTERACTIONS IN SWEPT WING FLOWS

Nabil M. El-Hady

Department of Mechanical Engineering and Mechanics
Old Dominion University, Norfolk, Virginia 23508

Abstract

An analysis is presented that examines the modulation of different instability modes satisfying the triad resonance condition in time and space in a three dimensional boundary-layer flow. Detuning parameters are used for the wavenumbers and the frequencies. The nonparallelism of the mean flow is taken into account in the analysis. At the leading-edge region of an infinite swept wing, different resonant triads are investigated that are comprised of traveling crossflow, stationary crossflow, vertical vorticity, and Tollmien-Schlichting modes. The spatial evolution of the resonating triad components are studied.

I. Introduction

An important stage in the transition from laminar to turbulent flow is a region of nonlinear development, characterized by a broad spectrum of nonlinearly interacting disturbances. The character of the nonlinear development is strongly dependent on the initial spectrum of the disturbances.

Most theoretical and experimental work was performed using the Blasius boundary layer to investigate the instability mechanism that break down into turbulence. On the other hand, little is known about the physical phenomena that leads to transition in cases like swept wings where the boundary layer is three-dimensional (3D). In this situation, the boundary-layer profile consists of a streamwise velocity component in the direction of the external inviscid flow and a crossflow velocity component normal to it along the wing surface. Due to that, different types of instability modes may exist and different possible interactions may occur between these modes resulting in stability characteristics that is much different from what linear theory would suggest.

The resonant interaction of three waves is considered one of the mechanisms that play an important role in determining the nonlinear characteristics of the development of disturbances, leading to transition. Such resonance occurs whenever the real wavenumbers k and frequencies ω satisfy the conditions

$$k_1 \pm k_2 \pm k_3 = 0, \quad \omega_1 \pm \omega_2 \pm \omega_3 = 0$$

with corresponding signs being taken.

In Blasius boundary layer, there usually exist triads comprised of two-dimensional wave propagating in the flow direction and two-obliquely propagating plane waves. Raetz[1,2] and Stuart[3] established the occurence of triad resonances for certain neutrally linear stable waves. Craik[4-7] examined the occurence of this triad resonance for certain unstable waves over a flat plate. Lekoudis[8] derived the nonlinear spatial and temporal evolution equations of the triad waves by relaxing Craiks assumption of perfect resonance. The resonance model of wave interaction is one of the experimentally observed phenomena (e.g., Kachanov et al.[9], Kachanov and Levechenko[10], Saric and Thomas[11], Saric et al.[12]), in two-dimensional flows that play an important role in the 3D secondary instability that break down into turbulence.

However, in 3D boundary layers, as on a swept wing, the triad is comprised of three resonantly interacting 3D waves that may propagate in different directions. Because 3D boundary layers are usually rich in instability modes, one expects the possible evolution of different triads with different interacting modes that resonate. Lekoudis[13] confirmed the existence of a triad on a swept wing that consists of three unsteady crossflow modes, but the interaction coefficients and the amplitudes of the interacting waves were never calculated in 3D boundary-layer flows.

It is known that transition prediction methods used for modern LFC transport depend primarily on the use of the e^n criterion. This method is based only on the exponential growth of small individual disturbances within a boundary layer according to linear stability theory. With the interaction of the linear modes of these disturbances and the possibility of rapid growth of

their amplitudes, as is the case for Blasius boundary layers[14,15], the e^n criterion is no longer valid and a modified one is needed.

In this article, we investigate the evolution of resonant triads in 3D boundary layers. The triads investigated are comprised of different instability modes, stationary crossflow (CF), traveling crossflow, vertical vorticity (VV), and Tollmien-Schlishting (TS) modes. In section II the nonlinear analysis of the triad resonant interaction is developed. The mean flow used in the calculations is the boundary layer on a modern LFC transonic 23° swept wing. In our analysis the growth of the boundary layer is taken into account assuming that it is of the same order as the nonlinear effects.[39] Details of the mean flow are given in section III. Section IV discusses the numerical procedures. Results for different mode-mode interactions are given in section V for parallel flows, while nonparallel flow effects are discussed in section VI. Then we end with concluding remarks.

II. Nonlinear Analysis

We consider the nonlinear interaction of wave packets in a 3D incompressible boundary layer on a swept wing. The flow field is governed by the non-dimensional incompressible Navier-Stokes equations. The Cartesian coordinate system used has the x-axis in the direction of the normal chord, the z-axis along the span, and the y-axis normal to the surface. The Reynolds number $R = U_e^* L^*/\nu_e^*$ is based on a reference length $L^* = (\nu_e^* s^*/U_e^*)^{1/2}$, where s^* is is the distance along the airfoil surface surface, and ν_e^* is the kinematic viscosity coefficient evaluated at the edge of the boundary layer.

The mean flow is assumed to be slightly nonparallel, with ε a small parameter characterizing the flow divergence, and identified with 1/R. The

method of multiple scales[16] is used to introduce the slow scales $(x_1,z_1,t_1) \equiv (\varepsilon x,\varepsilon z,\varepsilon t)$ that govern the growth of the boundary layer, the modulation of the disturbance amplitude, and the change in the eigenfunction. While the phase of the disturbance changes over the scales x, z, and t.

To determine the wave packet solution of the governing equations, we assume that the flow quantities possess uniformly valid expansions in the form,

$$\hat{u} = U(x_1,y,z_1) + \sum_{n=1}^{2} \varepsilon^n u_n(x,x_1,y,z,z_1,t,t_1) + O(\varepsilon^3) \tag{1}$$

$$\hat{v} = \varepsilon V(x_1,y,z_1) + \sum_{n=1}^{2} \varepsilon^n v_n(x,x_1,y,z,z_1,t,t_1) + O(\varepsilon^3) \tag{2}$$

$$\hat{w} = W(x_1,y,z_1) + \sum_{n=1}^{2} \varepsilon^n w_n(x,x_1,y,z,z_1,t,t_1) + O(\varepsilon^3) \tag{3}$$

$$\hat{p} = P(x_1,z_1) + \sum_{n=1}^{2} \varepsilon^n p_n(x,x_1,y,z,z_1,t,t_1) + O(\varepsilon^3) \tag{4}$$

Where U, V, W, and P are the steady mean-flow quantities and u, v, w, and p are the unsteady small disburbances. To account for the simultaneous effects of the flow divergence and the disturbance nonlinearity, we assume that both effects can be expressed by the same expansion parameter ε.

Substituting equations (1) - (4) into the governing Navier-Stokes equations after transforming the time and space derivatives, subtracting the mean-flow terms, and equating the coefficients of like powers of ε, we obtain,

Order ε:

$$L_1(u_1,v_1,w_1) = \frac{\partial u_1}{\partial x} + \frac{\partial v_1}{\partial y} + \frac{\partial w_1}{\partial z} = 0 \tag{5}$$

$$L_2(u_1,v_1,p_1) = \frac{\partial u_1}{\partial t} + U\frac{\partial u_1}{\partial x} + \frac{\partial U}{\partial y}v_1 + W\frac{\partial u_1}{\partial z} + \frac{\partial p_1}{\partial x} - R^{-1}\nabla^2 u_1 = 0 \tag{6}$$

$$L_3(v_1,p_1) = \frac{\partial v_1}{\partial t} + U\frac{\partial v_1}{\partial x} + W\frac{\partial v_1}{\partial z} + \frac{\partial p_1}{\partial y} + R^{-1}\nabla^2 v_1 = 0 \tag{7}$$

$$L_4(v_1,w_1,p_1) = \frac{\partial w_1}{\partial t} + U\frac{\partial w_1}{\partial x} + \frac{\partial W}{\partial y}v_1 + W\frac{\partial w_1}{\partial z} + \frac{\partial p_1}{\partial z} - R^{-1}\nabla^2 w_1 = 0 \tag{8}$$

where

$$\nabla^2 = \frac{\partial^2}{\partial x^2} + \frac{\partial^2}{\partial y^2} + \frac{\partial^2}{\partial z^2}$$

Order ε^2:

$$L_1(u_2,v_2,w_2) = -\frac{\partial u_1}{\partial x_1} - \frac{\partial w_1}{\partial z_1} \tag{9}$$

$$L_2(u_2,v_2,p_2) = -\frac{\partial u_1}{\partial t_1} - U\frac{\partial u_1}{\partial x_1} - W\frac{\partial u_1}{\partial z_1} - \frac{\partial p_1}{\partial x_1} + 2R^{-1}\left(\frac{\partial^2 u_1}{\partial x \partial x_1} + \frac{\partial^2 u_1}{\partial z \partial z_1}\right)$$

$$- \left(u_1\frac{\partial u_1}{\partial x} + v_1\frac{\partial u_1}{\partial y} + w_1\frac{\partial u_1}{\partial z}\right) - \left[\frac{\partial U}{\partial x_1}u_1 + V\frac{\partial u_1}{\partial y} + \frac{\partial U}{\partial z_1}w_1\right] \tag{10}$$

$$L_3(v_2,p_2) = -\frac{\partial v_1}{\partial t_1} - U\frac{\partial v_1}{\partial x_1} - W\frac{\partial v_1}{\partial z_1} + 2R^{-1}\left(\frac{\partial^2 v_1}{\partial x \partial x_1} + \frac{\partial^2 v_1}{\partial z \partial z_1}\right)$$

$$- \left(u_1\frac{\partial w_1}{\partial x} + v_1\frac{\partial w_1}{\partial y} + w_1\frac{\partial v_1}{\partial z}\right) - \left[V\frac{\partial v_1}{\partial y} + \frac{\partial V}{\partial y}v_1\right] \tag{11}$$

$$L_4(v_2,w_2,p_2) = -\frac{\partial w_1}{\partial t_1} - U\frac{\partial w_1}{\partial x_1} - W\frac{\partial w_1}{\partial z_1} - \frac{\partial p_1}{\partial z_1} + 2R^{-1}\left(\frac{\partial^2 w_1}{\partial x \partial x_1} + \frac{\partial^2 w_1}{\partial z \partial z_1}\right)$$

$$- \left(u_1\frac{\partial w_1}{\partial x} + v_1\frac{\partial w_1}{\partial y} + w_1\frac{\partial w_1}{\partial z}\right) - \left[\frac{\partial W}{\partial x_1}u_1 + V\frac{\partial w_1}{\partial y} + \frac{\partial W}{\partial z_1}w_1\right] \tag{12}$$

Here, the leading order problem governs the linear wave in a parallel flow, while the higher order problem includes both nonparallel and nonlinear effects.

2a. First-order equations

Consider the nonlinear interaction that may exist among three wave packets centered at the frequencies ω_1, ω_2, and ω_3. Thus we express the solution of equations (5) - (8) as a linear combination of three interacting waves according to,

$$q_{1m} = \sum_{n=1}^{3} a_n(x_1,z_1,t_1)\, \zeta_{mn}(x_1,y,z_1) e^{i\theta_n} + c.c. \tag{13}$$

where $q_{1m}, m=1,\ldots 6$ stands for $u_1, \partial u_1/\partial y, v_1, w_1, \partial w_1/\partial y$, and p_1 respectively and

$$\frac{\partial \theta_n}{\partial x} = \alpha_n(x_1,z_1) \tag{14}$$

$$\frac{\partial \theta_n}{\partial z} = \beta_n(x_1,z_1) \tag{15}$$

$$\frac{\partial \theta_n}{\partial t} = -\omega_n, \quad n=1,2,3 \tag{16}$$

The phase functions θ_n are assumed to be continuously differentiable, that is

$$\frac{\partial \alpha_n}{\partial z_1} = \frac{\partial \beta_n}{\partial x_1} \tag{17}$$

The α_n and β_n are the complex wave numbers in the x and z directions given by $\alpha_n = \alpha_{nr} + i\alpha_{ni}$ and $\beta_n = \beta_{nr} + i\beta_{ni}$, and ω_n are the complex frequencies given by $\omega_n = \omega_{nr} + i\omega_{ni}$. They satisfy the resonance conditions,

$$\omega_{3r} - \omega_{1r} - \omega_{2r} = \varepsilon\sigma_t \tag{18}$$

$$\alpha_{3r} - \alpha_{1r} - \alpha_{2r} = \varepsilon\sigma_x \tag{19}$$

$$\beta_{3r} - \beta_{1r} - \beta_{2r} = \varepsilon\sigma_z \tag{20}$$

where the detuning parameters σ_t, σ_x and σ_z [all O(1)] are introduced to introduced to express quantitatively the nearness of the above resonance.

Substituting (13)-(16) into equations (5)-(8), separating coefficients for $e^{i\theta_n}$, n=1,2,3, and writing the result as six first-order systems of ordinary differential equations, we obtain,

$$D\zeta_{mn} - \sum_{j=1}^{6} (b_{mj})_n \zeta_{jn} = 0, \quad m=1,\ldots 6 \tag{21}$$

subject to the boundary conditions

$$\zeta_{1n} = \zeta_{3n} = \zeta_{4n} = 0 \qquad \text{at } y = 0 \tag{22}$$

$$\zeta_{1n}, \zeta_{3n}, \zeta_{4n} \to 0 \qquad \text{as } y \to \infty \tag{23}$$

where $D = d/dy$, and the nonzero coefficients of $(b_{mj})_n$ are given in Appendix A.

2b. Second-order equations

In order to determine the conditions for the elimination of secular terms in the second-order equations (9)-(12), and hence determine the amplitudes a_n in (13), we seek a particular solution for the second-order equations in the form,

$$q_{2m} = \sum_{n=1}^{3} \psi_{mn}(y;x_1,z_1,t_1)e^{i\theta_n} + c.c. \tag{24}$$

where q_{2m}, m=1,...6, stands for $u_2, \partial u_2/\partial y, v_2, w_2, \partial w_2/\partial y$ and p_2, respectively. Substituting (13)-(20) and (24) into (9)-(12) and separating the coefficients of $e^{i\theta_n}$, n=1,2,3, we obtain three separate systems of equations, where each can be written as six first-order sets of equations in the form,

$$D\psi_{mn} - \sum_{j=1}^{6} (b_{mj})_n \psi_{jn} = I_{mn}, \quad m=1,\ldots 6 \tag{25}$$

subject to the boundary conditions,

$$\psi_{1n} = \psi_{3n} = \psi_{4n} = 0 \qquad \text{at } y = 0 \tag{26}$$

$$\psi_{1n}, \psi_{3n}, \psi_{4n} \to 0 \qquad \text{as } y \to \infty \tag{27}$$

The coefficients $(b_{mj})_n$ are the same as in equation (21), while the inhomogeneous terms I_{mn} are functions of the first-order eigensolutions ζ_{mn} of equation (13), α_n, β_n, ω_n and the mean-flow quantities. The terms I_{mn} include all nonparallel and nonlinear effects.

Since the homogeneous parts of equation (25) are the same as in equation (21), and since the latter has a nontrivial solution, the inhomogeneous equation (25) has a solution if, and only if, and only if, the inhomogeneous parts are orthogonal to every solution of the corresponding adjoint homogeneous problem; that is,

$$\int_0^\infty \sum_{m=1}^{6} I_{mn} \zeta^*_{mn} dy = 0, \quad n=1,2,3 \tag{28}$$

where ζ^*_n are solutions of the adjoint problems, they are,

$$D\zeta^*_{mn} - \sum_{j=1}^{6} \tilde{(b_{mj})}_n \zeta^*_{jn} = 0, \quad m=1,\ldots 6 \tag{29}$$

$$\zeta^*_{2n} = \zeta^*_{4n} = \zeta^*_{5n} = 0 \qquad \text{at } y = 0 \tag{30}$$

$$\zeta^*_{2n}, \zeta^*_{4n}, \zeta^*_{5n} \to 0 \qquad \text{as } y \to \infty \tag{31}$$

for $n=1,2,3$, and $\tilde{b}_{mj} = -b_{jm}$.

The solvability conditions (28) give the following differential equations for the evolution of the amplitudes a_n in time and space,

$$h_{11} \frac{\partial a_1}{\partial t} + h_{21} \frac{\partial a_1}{\partial x} + h_{31} \frac{\partial a_1}{\partial z} + \varepsilon_1 h_{41} a_1 + \varepsilon_2 h_{51} \bar{a}_2 a_3 e^{-\Gamma_1} = 0 \tag{32}$$

$$h_{12}\frac{\partial a_2}{\partial t} + h_{22}\frac{\partial a_2}{\partial x} + h_{32}\frac{\partial a_2}{\partial z} + \varepsilon_1 h_{42} a_2 + \varepsilon_2 h_{52}\bar{a}_1 a_3 e^{-\Gamma_2} = 0 \tag{33}$$

$$h_{13}\frac{\partial a_3}{\partial t} + h_{23}\frac{\partial a_3}{\partial x} + h_{33}\frac{\partial a_3}{\partial z} + \varepsilon_1 h_{43} a_3 + \varepsilon_2 h_{53} a_1 a_2 e^{-\Gamma_3} = 0 \tag{34}$$

where h_{1n}, h_{2n}, h_{3n}, h_{4n}, h_{5n}, and Γ_n are given in Appendix B, and $(\bar{\ })$ indicates a complex conjugate of $(\bar{\ })$.

Equations (32)-(34) account for the combined effect of the growth of the boundary layer, and the nonlinear interactions. The parameters ε_1 and ε_2 are shown here ($\varepsilon_1 = \varepsilon_2 = \varepsilon$ in the analysis) only to indicate terms due to each effect. If $\varepsilon_2 << \varepsilon_1$, the nonlinear interaction can be neglected. When $\varepsilon_1 << \varepsilon_2$, the nonparallel effect can be neglected. It is worth noting that with this formulation both nonlinear and nonparallel effects are independent of the particular disturbance quantity being considered.

Solution of equations (32)-(34) for a general initial condition is not a simple task. However, by assuming the spatial modulation of a single frequency disturbance on an infinite span wing, a situation closer to experiments[17,18], we can allow for modulation only in the x-direction, and equations (32)-(34) can be simplified by

$$\frac{\partial}{\partial t} = \frac{\partial}{\partial z} = 0 \tag{35}$$

$$\omega_{3r} - \omega_{1r} - \omega_{2r} = 0, \quad \sigma_t = 0 \tag{36}$$

$$\beta_{3r} - \beta_{1r} - \beta_{2r} = 0, \quad \sigma_z = 0 \tag{37}$$

It is convenient to introduce the transformation

$$A_n = \varepsilon a_n \exp\left(-\int \alpha_{ni} dx - \beta_{ni} z\right) \tag{38}$$

then equations (32)-(34) reduce to

$$\frac{dA_1}{dx} = (G_1 - \alpha_{1i})A_1 + H_1 \bar{A}_2 A_3 e^{i\phi} \tag{39}$$

$$\frac{dA_2}{dx} = (G_2 - \alpha_{2i})A_2 + H_2\bar{A}_1 A_3 e^{i\phi} \tag{40}$$

$$\frac{dA_3}{dx} = (G_3 - \alpha_{3i})A_3 + H_3 A_1 A_2 e^{-i\phi} \tag{41}$$

where

$$G_n = -\varepsilon\frac{h_{4n}}{h_{2n}}, \tag{42}$$

$$H_n = -\frac{h_{5n}}{h_{2n}}, \tag{43}$$

$$\phi = \int \varepsilon\sigma_x dx \tag{44}$$

In equations (38), β_{ni} is a parameter and is made equal to zero in equations (39)-(41). We note that for the case of an infinite span wing, if the initial wave has $\beta_i = 0$, it will remain zero downstream.

In order that the interaction coefficients H_n and the wave amplitudes A_n are uniquely defined, it is necessary to specify the normalization imposed on the eigensolutions ζ_{mn} of the first-order problem. This is chosen such that the maximum of the r.m.s. of $\zeta_{1n}(\zeta_{1n} \equiv u_n)$ over y is equal to one. Note that the nonparallel coefficients G_n do not depend on the normalization of ζ_{mn} or ζ^*_{mn}.

To derive real equations for the amplitudes and phases, we let,

$$A_n = \frac{1}{2}A_n^* e^{i\lambda_n} \tag{45}$$

$$G_n = G_n^* e^{i\chi_n} \tag{46}$$

$$H_n = H_n^* e^{i\tau_n}, \quad n=1,2,3 \tag{47}$$

Substituting (45)-(47) into (39)-(41) and dropping the *, we obtain,

$$\frac{dA_1}{dx} = (G_1 \cos\chi_1 - \alpha_{1i})A_1 + \frac{1}{2}H_1 A_2 A_3 \cos(\gamma + \tau_1 + \phi) \tag{48}$$

$$\frac{dA_2}{dx} = (G_2 \cos \chi_2 - \alpha_{2i})A_2 + \frac{1}{2}H_2 A_1 A_3 \cos (\gamma + \tau_2 + \phi) \tag{49}$$

$$\frac{dA_3}{dx} = (G_3 \cos \chi_3 - \alpha_{3i})A_3 + \frac{1}{2}H_3 A_1 A_2 \cos (-\gamma + \tau_3 - \phi) \tag{50}$$

$$\frac{d\gamma}{dx} = (G_3 \sin \chi_3 - G_2 \sin \chi_2 - G_1 \sin \chi_1) + [H_3 \frac{A_1 A_2}{2A_3} \sin (-\gamma + \tau_3 - \phi)$$

$$- H_2 \frac{A_1 A_3}{2A_2} \sin (\gamma + \tau_2 + \phi) - H_1 \frac{A_2 A_3}{2A_1} \sin (\gamma + \tau_1 + \phi)] \tag{51}$$

where

$$\gamma = \lambda_3 - \lambda_2 - \lambda_1 \tag{52}$$

III. Mean Flow

The mean flow used in these calculations is the boundary layer with suction on a 23° swept infinite span wing. The airfoil section (designated SCLFC(1)-0513F) is supercritical with normal chord $c = 6.44$ ft. This wing was the subject of extensive experiments designed to examine supercritical laminar flow control technology at the Langley Research Center[19,20]. Linear stability calculations for this wing have been given by El-Hady[21,22], Mack[23], and Berry et al.[24]

Freestream conditions for the present calculations are Mach number = 0.82 and a chord Reynolds number of 20×10^6. The upper surface pressure coefficient distribution is shown in Fig. (1) together with the suction parameter distribution, and the distribution of the boundary layer maximum crossflow component $|V_N|$ maximum along the chord.

The three-dimensional boundary-layer solution is calculated using a boundary layer program that is adapted from the code of Kaups and Cebeci[25] for laminar, compressible boundary layers with adiabatic and wall suction boundary conditions. The code assumes zero pressure gradient along the wing generator.

IV. Numerical Procedures

For $n = 1$, 2, and 3, the set of equations (21)-(23) and their adjoints (29)-(31) can be solved analytically in the freestream at $y = y_e$, producing three linearly independent, exponentially decaying solutions with the characteristic values,

$$\Lambda_1 = -(\alpha_n^2 + \beta_n^2)^{1/2} \tag{53}$$

$$\Lambda_2 = -[\alpha_n^2 + \beta_n^2 + iR(\alpha_n + W_e\beta_n - \omega_n)]^{1/2} \tag{54}$$

$$\Lambda_3 = \Lambda_2 \tag{55}$$

with the freestream solution as initial condition, equation (21) is integrated from $y = y_e$ to $y = 0$ at the wall, using a variable step-size algorithm[26], based on the Runge-Kutta-Fehlburg fifth-order forumlas. The solution is orthonormalized at a preselected set of points using a modified Gram-Schmidt procedure. A Newton-Raphson technique is used to iterate on the eigenvalue to satisfy the last wall boundary condition. The eigensolutions associated with the adjoint problem can be determined by integrating equations (29)-(31) using the same procedures and the same previously determined eigenvalues.

To evaluate the nonparallel terms $\partial\zeta_{mn}/\partial x_1$ and $d\alpha_n/dx_1$, for $n = 1$, 2, and 3, we differentiate the first-order problem (21) with respect to x_1 and obtain,

$$D\left(\frac{\partial\zeta_{mn}}{\partial x_1}\right) - \sum_{j=1}^{6} (b_{mj})_n \frac{\partial\zeta_{jn}}{\partial x_1} = \sum_{j=1}^{6} \frac{\partial(b_{mj})_n}{\partial x_1}\zeta_{jn}, \quad m = 1,\ldots 6 \tag{56}$$

$$\frac{\partial\zeta_{1n}}{\partial x_1} = \frac{\partial\zeta_{3n}}{\partial x_1} = \frac{\partial\zeta_{4n}}{\partial x_1} = 0 \qquad \text{at } y = 0 \tag{57}$$

$$\frac{\partial\zeta_{1n}}{\partial x_1}, \frac{\partial\zeta_{3n}}{\partial x_1}, \frac{\partial\zeta_{4n}}{\partial x_1} \to 0 \qquad \text{as } y \to \infty \tag{58}$$

The homogeneous parts of equation (56) have a nontrivial solution. Their eigenvalues and adjoint are the same as those for the first-order problem (21). Then, by applying the solvability condition, we obtain,

$$\frac{d\alpha_n}{dx_1} = -\frac{h_{6n}}{ih_{2n}}, \quad n = 1, 2, 3 \tag{59}$$

where h_{6n} are given in quadratures in terms of ζ_{mn}, ζ^*_{mn}, α_n, and β_n (see Appendix C). Condition (59) permits the integration of equations (56)-(58) to determine $\partial\zeta_{mn}/\partial x_1$ using the same procedures as those for the first-order problem, but for nonhomogeneous sets of equations.

With all terms in h_{2n} and h_{4n} known, the nonparallel coefficients G_n are calculated from equation (42), separately for each wave (n = 1, 2, and 3). Whereas the interaction coefficients H_n are calculated from equation (43) using the parallel results for the three waves altogether.

The calculations are repeated at different streamwise locations to evaluate G_n and H_n for given waves of fixed physical frequency f in Hz, and fixed physical spanwise wavelength λ_z (nondimensionalized with respect to the normal chord c) that satisfy the conditions (36) and (37). For different initial amplitudes of the respective waves, the amplitude evolution equations (48)-(51) are then integrated using a fourth-order variable interval Runge-Kutta method by Fehlberg[27].

V. Nonlinear Effects in Parallel Flows

When the amplitude of the disturbance, although small, is sufficiently large, nonparallel effects are thought to have no substantial influence. In this section, we assume that $\varepsilon_1 << \varepsilon_2$ such that nonparallel effects are neglected.

5a. Interaction between traveling CF modes

First, we study a triad that is comprised of traveling CF waves near the leading edge of the swept wing. The triad has the frequencies $f_1 = 100$ Hz, $f_2 = 200$ Hz, and $f_3 = 300$ Hz. The corresponding spanwise wavelengths are $\lambda_z = 0.0006$, 0.0006, and 0.0003, respectively. Calculations start at $R = 260$ (0.078% chord) where the three waves are unstable in the absence of the interaction. The frequencies and spanwise wavelengths satisfy the resonant conditions (36) and (37) at all streamwise locations.

When the initial amplitudes of the triad waves are comparable in magnitude, the interaction between the waves is found to be very weak (not shown). It is also found that the initial spectrums of the triad amplitudes and phases play an important role in the interaction process. For example, Fig. (2) shows the modulation with R of both A_3 and the phase angle γ defined by equation (52). The initial amplitude $A_{30} = 0.0001$, and the initial phase angle $\gamma_0 = 0$ (all calculations are for $\gamma_0 = 0$ unless otherwise stated). For $(A_{10} = A_{20}) < 0.0001$, the amplitude A_3 is hardly affected by the interaction. With the increase of A_{10} and A_{20}, a sharp increase in A_3 occurs starting at an earlier streamwise location. Fig. (3) shows the modulation of A_3 for the same conditions as in Fig. (2) but for $\gamma_0 = \pi$. In both cases the modulation of A_1 and A_2 is almost unaffected by the interaction. Fig. (4) shows that the modulation of A_3 is affected by its initial amplitude. If A_{30} is large, A_3 is hardly affected by the interaction, until later downstream after the amplitudes A_1 and A_2 become large enough. While for small A_{30}, the effect of the interaction shows up early upstream with a very sharp increase.

A strong interaction may also occur and amplify A_1 or A_2 depending on the appropriate initial amplitude and phase spectrum. Fig. (5) shows strong

modulation of A_1 when A_{10} is very small compared to A_{20} and A_{30}. The same picture is almost true for the modulation of A_2 when A_{20} is very small compared to A_{10} and A_{30}. In both situations A_3 undergoes weak variations from its linear modulation (not shown). Fig. (6) gives the dependence of A_1 on the initial amplitude A_{10} when $A_{20} = 0.0005$, and $A_{30} = 0.002$.

Fig. (7) shows the variation with R of the interaction coefficients H_n, n = 1, 2, and 3, given by equation (43). It shows that $|H_n|$, corresponding to $f_3 = 300$ Hz and $\lambda_z = 0.0003$, is much higher than those for f_1 and f_2.

Fig. (8) shows the variation of the detuning parameter $\varepsilon\sigma_x$ with R. It indicates that perfect tuning occurs only at one location. In spite of that, preceding results show that a strong interaction continues to exist even if the resonant conditions are not tuned provided that the initial amplitudes have the appropriate spectrum.

As we see from previous calculations, the triad used for this study exhibits a strong resonance that may amplify a superharmonic (A_3), or may amplify a subharmonic (A_1 or A_2). This is again illustrated in Fig. (9). At a sufficient distance downstream, the domination of one or the other will depend on the spectrum of the initial amplitudes of the interacting waves. These results may explain the anomalies found in the crossflow observations of Saric and Yeates[28]. In spite of the 1-cm space streaks they visually observed, their hot wire measurements in the boundary layer showed a superharmonic of 0.5-cm periodicity dominated disturbance growth. Reed[29] explained this anomalies using an approach that considered the growth of the superharmonic as a secondary instability in the presence of finite amplitude unsteady crossflow disturbance. The triad resonance model presented here

predicts that a superharmonic (λ_z = 0.0003) will amplify and its amplitude ratio will eventually reach three times or more the amplitude of other components of the triad (λ_z = 0.0006, λ_z = 0.0006) when the initial amplitude of the superharmonic is very small. The same model also predicts that a subharmonic (λ_z = 0.0006) may dominate disturbance growth if its intial amplitude is small compared to other components of the triad.

5b. Interaction between traveling CF and VV modes

In a three-dimensional boundary layer, the disturbance is necessarily three dimensional. At the leading edge region of a swept wing and in the direction of crossflow, there are really two spectra to be considered to the solution of the leading-order equations (21). Crossflow modes (stationary or traveling) are given by the eigensolution of equation (21). The same equations also admit eigensolutions with $v = 0$ and $p = 0$, correspond physically to horizontal motions which are called vertical vorticity eigenmodes. These eigenmodes, as in the case of two-dimensional flows[30-33], are always damped but the damping rate may be quite small so that the nonlinear effect could trigger large instabilities[32,33].

In our calculations, we were able to converge to a VV mode in the crossflow direction, that is damped.

Here, we study the resonant interaction of a triad that is comprised of two traveling CF modes (f_1 = 100 Hz, λ_z = 0.0006 and f_2 = 200 Hz, λ_z = 0.0006) and a VV mode (f_3 = 300 Hz, λ_z = 0.0003). Calculations start at R = 779 (2.1% chord), where, in the absence of the interaction, the CF modes are unstable while the VV mode is damped. Again, the frequencies and spanwise wavelengths satisfy the resonant conditions (36) and (37) at all streamwise locations.

Fig. (10) shows that a VV mode with $A_{30} = 0.0001$ resonate with two traveling CF modes and becomes strongly unstable in a short distance downstream. Fig. (11) shows the influence of A_{30} on this instability when the CF mode initial amplitudes $A_{10} = A_{20} = 0.002$. This strong instability may be due to a strong interaction coefficent $|H_3|$ (corresponding to the VV mode) compared to $|H_1|$ and $|H_2|$, see Fig. (12). This strong instability of the VV mode occurs in spite of the imperfect resonant conditions shown by the distribution of the detuning parameter $\varepsilon\sigma_x$ in Fig. (13).

5c. Interaction between traveling CF and stationary CF modes

Here, we study the resonant interaction that is comprised of two traveling CF modes ($f_2 = 300$ Hz, $\lambda_z = 0.0006$ and $f_3 = 300$ Hz, $\lambda_z = 0.0003$) and a stationary CF mode ($f_1 = 0$, $\lambda_z = 0.0006$) near the leading edge of the swept wing. Calculations start at $R = 260$ (0.078% chord) where the three waves are unstable in the absence of the interaction. The frequencies and spanwise wavelengths satisfy the resonant conditions (36) and (37) at all streamwise locations.

Fig. (14) shows the effect of the stationary CF vortex with initial amplitude $A_{10} = 0.005$ on traveling CF modes A_2 and A_3. Since all waves are unstable in the range of Reynolds number considered, the interaction process seems to accelerate the growth of A_2 and A_3 compared to their linear growth. The detuning parameter $\varepsilon\sigma_x$ distribution is given in Fig. (15). Fig. (16) gives the effect of the initial amplitude of the stationary vortex on the modulation of A_2 and A_3.

5d. Interaction between TS and stationary CF modes

This type of interaction is a major unanswered question concerning swept-wing flows. Some type of interaction between a crossflow vortex and

amplifying TS mode is thought to cause premature transition on a swept wing. Saric and Reed[34] suggested that the anomaly behavior of transition in the early LFC work of Bacon et al.[35] when sound is introduced in the presence of crossflow vortices can be due to this interaction phenomenon. Also, the experimental work of Poll[36] on yawed cylinders and of Michel et al.[37] on an infinite swept wing, observed unsteadiness at transition which might also be due to this interaction phenomenon. Reed[40], using a parametric resonance model, showed that CF vortices could excite TS modes in the three-dimensional boundary layer on the X-21 wing, producing a double exponential growth of the TS mode.

Here, we study one of these possible interactions. In the absence of the interaction, a crossflow vortex ($f_1 = 0$ and $\lambda_z = 0.003$) starts to amplify nearly at $R = 706$ (1.6% chord), then experiences a very slow growth for a long distance downstream, until it dies approximately at $R = 1663$ (13% chord). Two TS modes having the same frequency ($f_2 = 20$ KHz, $\lambda_z = 0.012$ and $f_3 = 20$ KHz, $\lambda_z = 0.0024$) will amplify shortly after $R = 706$ and both decay around $R = 1150$ (5.8% chord). The frequencies and spanwise wavelengths of the triad satisfy the resonant conditions (36) and (37) at all streamwise locations.

For different values of the initial amplitude of the crossflow vortex, Fig. (17) shows large amplification of the TS modes A_2 and A_3 due to the interaction, when A_{20} and A_{30} are small ($A_{20} = A_{30} = 0.0001$). The figure also shows a reduction in the vortex amplitude due to the interaction. Higher values of the initial TS amplitudes weaken the interaction as shown in Fig. (18) for a CF vortex initial amplitude $A_{10} = 0.1$.

Fig. (19) shows the change in the interaction coefficients with R, where $|H_3|$ and $|H_2|$ (corresponding to TS modes) are higher than $|H_1|$. Fig. (20) shows the distribution of the detuning parameter $\varepsilon\sigma_x$ with R.

The effect of the initial value of the phase angle γ_0 is given in Fig. (21) for $A_{10} = 0.1$, $A_{20} = A_{30} = 0.0001$. The anomaly behavior of A_3 at the beginning of the interaction is due to different values of γ_0. Fig. (22) shows how γ reaches the same value at some distance downstream in spite of different initial values γ_0.

VI. Nonparallel Flow Effects

When $\varepsilon_1 = \varepsilon_2$, nonparallelism of the mean flow comes into play significantly in the nonlinear amplitude modulation. However, the nonparallel terms in equations (48)-(51) turn out to be most important as the disturbance first grows and this, in turn, controls what happens subsequently as the amplitude of the disturbance increases. Only the interaction between TS and stationary CF modes is investigated in this section.

Fig. (23) shows the linear parallel and nonparallel amplitude modulations of the same instability modes given in section 5d. Fig. (24) shows the nonlinear modulation of the amplitudes with the nonparallelism of the mean flow included for various initial amplitudes of the interacting modes. This figure indicates that during the initial growth or decay of the amplitude, its modulation follows exactly the nonparallel development until the amplitudes are large enough to interact nonlinearly.

VII. Concluding Remarks

1. The preceding calculations show that the development of many triads, whose components can, in principle, take part in several resonant interactions at once, occurs in three-dimensional flows of boundary-layer type.

2. An important role in the nonlinear process is played by the initial spectrum of amplitude and phases of the triad components.

3. Due to the interaction of different instability modes, even if they are not strongly amplified, the classification concept suggested by Pfenninger[38] for the stability problem into independent modes is no longer valid.

4. Nonparallel flow effects control the initial development of the disturbance triad components while the disturbance amplitude is sufficiently small. As the amplitudes increase, nonlinear effects control their subsequent spatial development.

5. The above analysis becomes incorrect with the increase of the amplitudes A_n, but the nature of a set of phenomena in the 3D boundary layers is connected to the resonant mechanism, and may be explained on the basis of the results.

Acknowledgement

This work was supported by the NASA Langley Research Center under Grant No. NAG1-729.

References

1. Raetz, G. S., A New Theory of the Case of Transition in Fluid Flows. Norair Rep, NOR-59-383, Hawthorne, CA, 1959.

2. Raetz, G. S., Current Status of Resonance Theory of Transition. Norair Rep. NOR-64-111, Hawthorne, CA, 1964.

3. Stuart, J. T., On Three-Dimensional Non-Linear Effects in the Stability of Parallel Flows. Advances in Aerospace Sciences, Vol. 3, 1961, pp. 121-142.

4. Craik, A. D. D., Nonlinear Resonant Instability in Boundary Layers. J. Fluid Mech., Vol. 50, 1971, pp. 393-413.

5. Craik, A. D. D., Second Order Resonance and Subcritical Instability. Proc. Roy. Soc., London, Vol. A343, 1975, pp. 351-362.

6. Craik, A. D. D., Evolution in Space and Time of Resonant Wave Triads. II. A Class of Exact Solutions. Proc. Roy. Soc., London, Vol. A363, 1978, pp. 257-269.

7. Craik, A. D. D., Wave Interactions and Fluid Flows. Cambridge University Press, Cambridge, 1985.

8. Lekoudis, S. G., On the Triad Resonance in the Boundary Layer. Lockheed-Georgia Company Report No. LG77ER0152, 1977.

9. Kachanov, Yu. S., Kozlov, V. V. and Levchenko, V. Ya., Nonlinear Development of a Wave in a Boundary Layer. Fluid Dynamics, Vol. 3, 1977, pp. 383-390.

10. Kachanov, Yu. S. and Levchenko, V. Ya., The Resonant Interaction of Disturbances at Laminar-Turbulent Transition in a Boundary Layer. J. Fluid Mech., Vol. 138, 1984, pp. 209-247.

11. Saric, W. S. and Thomas, A. S. W., Experiments on the Subharmonic Route to Transition. Turbulent and Chaotic Phenomena in Fluids, ed. T. Tatsumi, North-Holand, 1984.

12. Saric, W. S., Kozlov, V. V. and Levchenko, V. Ya., Forced and Unforced Subharmonic Resonance in Boundary-Layer Transition. AIAA Paper No. 84-0007, 1984.

13. Lekoudis, S. G., Resonant Wave Interactions on a Swept Wing. AIAA J., Vol. 18, 1980, pp. 122-124.

14. Volodin, A. G. and Zel'man, M. B., Three-Wave Resonance Interaction of Disburbances in a Boundary Layer. Fluid Dynamics, Vol. 13, 1979, pp. 698-703.

15. Nayfeh, A. H. and Bozatli, A. N., Nonlinear Wave Interaction in Boundary Layers, AIAA Paper 79-1496, 1979.

16. Nayfeh, A. H., Perturbation Methods. Wiley-Interscience, 1973.

17. Arnal, D. and Juillen, J. C., Three-Dimensional Transition Studies at ONERA/CERT. AIAA Paper No. 87-1335, 1987.

18. Bippes, H. and Nitschke-Kowsky, P., Experimental Study of Instability Modes in a Three-Dimensional Boundary Layer. AIAA Paper No. 87-1336, 1987.

19. Pfenninger, W., Reed, H. L. and Dagenart, J. R., Design Considerations of Advanced Supercritical Low-Drag Suction Airfoils. Viscous Drag Reduction, Vol. 72, Progress in Astronautics and Aeronautics, 1980.

20. Harvey, W. D. and Pride, J. D., The NASA Langley Laminar Flow Control Experiment. AIAA Paper No. 82-0567, 1982.

21. El-Hady, N. M., On the Stability of Three-Dimensional Compressible Nonparallel Boundary Layers. AIAA Paper No. 80-1374, 1980.

22. El-Hady, N. M., On the Effect of Boundary Layer Growth on the Stability of Compressible Flows. NASA CR-3474, 1981.

23. Mack, L. M., Compressible Boundary-Layer Stability Calculations for Sweptback Wings with Suction. AIAA Paper No. 81-0196, 1981.

24. Berry, S. A., Dagenhart, J. R., Viken, J. K. and Yeaton, R. B., Boundary-Layer Stability Analysis of NLF and LFC Experimental Data at Subsonic and Transonic Speeds. SAE Technical Paper No. 871859,1987.

25. Kaups, K. and Cebeci, T., Compressible Laminar Boundary Layers with Suction on Swept and Tapered Wings. J. Aircraft, Vol. 14, 1977.

26. Scott, M. R. and Watts, H. A., Computational Solution of Linear Two-Point Boundary Value Problems via Orthonormalization. SIAM J. Numer. Anal., Vol. 14, 1977, pp. 40-70.

27. Hull, T. E., Enright, W. H., Fillen, B. M. and Sedgwick, A. E., Comparing Numerical Methods for Ordinary Differential Equations. SIAM J. for Num. Anal., Vol. 9, 1972, pp. 603-637.

28. Saric, W. S. and Yeates, L. G., Generation of Crossflow Vortices in a Three-Dimensional Flat-Plate Flow. Proceedings of 2nd IUTAM Symposium on Laminar-Turbulent Transition, Novosibirsk, USSR, July 9-13, 1984, Springer-Verlag.

29. Reed, H., Disturbance-Wave Interactions in Flow with Crossflow. AIAA Paper No. 85-0494, 1985.

30. Gustavsson, L. H. and Hultgren, L. S., A Resonance Mechanism in Plane Coutte Flow. J. Fluid Mech., Vol. 98, 1980, pp. 149-159.

31. Benny, D. J. and Gustavsson, L. H., A New Mechanism for Linear and Nonlinear Hydrodynamic Instability. Studies in Appl. Math., Vol. 64, 1981, pp. 185-209.

32. Herbert, Th., Subharmonic Three-Dimensional Disturbances in Unstable Plane Shear Flows. AIAA Paper No. 83-1759, 1983.

33. Nayfeh, A. H., Three-Dimensional Spatial Instability in Boundary-Layer Flows. AIAA Paper No. 85-1697, 1985.

34. Saric, W. S. and Reed, H., Three-Dimensional Stability of Boundary Layers. Proc. Perspectives in Turbulence Symp., Gottingen, 11-15 May 1987, pp. 1-22.

35. Bacon, J. W., Jr., Pfenninger, W. and Moore, C. R., Influence of Acoustical Disturbances on the Behavior of a Swept Laminar Suction Wing. Northrup Report NOR-62-124, 1962.

36. Poll, D. I. A., Some Observations of the Transition Process on the Windward Face of a Long Yawed Cylinder. J. Fluid Mech., Vol. 150, 1985.

37. Michel, R., Arnal, D., Coustols, E., and Juillen, J. C., Experimental and Theoretical Studies of Boundary-Layer Transition on a Swept Infinite Wing. Laminar-Turbulent Transition, ed. V. V. Kozlov, Springer-Verlag, 1985, pp. 329-356.

38. Pfenninger, W., Laminar Flow Control - Laminarization. AGARD Report No. 654, Special Course in Drag Reduction, 1977.

39. Hall, P. and Smith, F. T., On the Effects of Nonparallelism, Three Dimensionality, and Mode Interaction in Nonlinear Boundary-Layer Stability. Studies in Appl. Math., Vol. 70, 1984, pp. 91-182.

40. Reed, H., Wave Interactions in Swept-Wing Flows. AIAA Paper No. 84-1678, 1984.

Appendix A

$$b_{12} = 1,\ b_{21} = iR(U\alpha_n + W\beta_n - \omega_n) + \alpha_n^2 + \beta_n^2$$

$$b_{23} = R\ DU,\ b_{26} = iR\alpha_n,\ b_{31} = -i\alpha_n$$

$$b_{34} = -i\beta_n,\ b_{45} = 1,\ b_{53} = R\ DW,$$

$$b_{54} = b_{21},\ b_{56} = iR\beta_n,\ b_{62} = b_{31}R^{-1}$$

$$b_{63} = -b_{21}R^{-1},\ b_{65} = b_{34}R^{-1},\ \text{and } n = 1,\ 2,\ 3$$

Appendix B

$$h_{1n} = \int_0^\infty [R\zeta_{1n}\zeta_{2n}^* + R\zeta_{4n}\zeta_{5n}^* - \zeta_{3n}\zeta_{6n}^*]dy \tag{B1}$$

$$h_{2n} = \int_0^\infty [R(X_n\zeta_{1n} + \zeta_{6n})\zeta_{2n}^* - \zeta_{1n}\zeta_{3n}^* + RX_n\zeta_{4n}\zeta_{5n}^* - (R^{-1}\zeta_{2n} + X_n\zeta_{3n})\zeta_{6n}^*]dy \tag{B2}$$

$$h_{3n} = \int_0^\infty [RZ_n\zeta_{1n}\zeta_{2n}^* - \zeta_{4n}\zeta_{3n}^* + R(Z_n\zeta_{4n} + \zeta_{6n})\zeta_{5n}^* - (R^{-1}\zeta_{5n} + Z_n\zeta_{3n})\zeta_{6n}^*]dy \tag{B3}$$

$$\begin{aligned} h_{4n} = \int_0^\infty \{ & R[X_n \frac{\partial\zeta_{1n}}{\partial x_1} + \frac{\partial\zeta_{6n}}{\partial x_1} - 2iR^{-1}\zeta_{1n}(\frac{\partial\alpha_n}{\partial x_1} + \frac{\partial\beta_n}{\partial z_1}) + \frac{\partial U}{\partial x_1}\zeta_{1n} + V\zeta_{2n} \\ & + \frac{\partial U}{\partial z_1}\zeta_{4n} + Z_n\frac{\partial\zeta_{1n}}{\partial z_1}]\zeta_{2n}^* - (\frac{\partial\zeta_{1n}}{\partial x_1} + \frac{\partial\zeta_{4n}}{\partial z_1})\zeta_{3n}^* + R[X_n\frac{\partial\zeta_{4n}}{\partial x_1} \\ & - 2iR^{-1}\zeta_{4n}(\frac{\partial\alpha_n}{\partial x_1} + \frac{\partial\beta_n}{\partial z_1}) + \frac{\partial\zeta_{6n}}{\partial z_1} + \frac{\partial W}{\partial x_1}\zeta_{1n} + V\zeta_{5n} + \frac{\partial W}{\partial z_1}\zeta_{4n} + Z_n\frac{\partial\zeta_{4n}}{\partial z_1}]\zeta_{5n}^* \\ & - [R^{-1}(\frac{\partial\zeta_{2n}}{\partial x_1} + \frac{\partial\zeta_{5n}}{\partial z_1}) + X_n\frac{\partial\zeta_{3n}}{\partial x_1} - 2iR^{-1}\zeta_{3n}(\frac{\partial\alpha_n}{\partial x_1} + \frac{\partial\beta_n}{\partial z_1}) + VD\zeta_{3n} + DV\zeta_{3n} \\ & + Z_n\frac{\partial\zeta_{3n}}{\partial z_1}]\zeta_{6n}^*\}dy \end{aligned} \tag{B4}$$

for n = 1, 2, and 3

$$h_{51} = \int_0^\infty \{-R[i(\bar{\alpha}_2 - \alpha_3)\bar{\zeta}_{12}\zeta_{13} - \zeta_{33}\bar{\zeta}_{22} - \bar{\zeta}_{32}\zeta_{23} + i\bar{\beta}_2\bar{\zeta}_{12}\zeta_{43} - i\beta_3\zeta_{13}\bar{\zeta}_{42}]\zeta^*_{21}$$

$$- R[i(\bar{\alpha}_2\bar{\zeta}_{42}\zeta_{13} - i\alpha_3\zeta_{43}\bar{\zeta}_{12} - \zeta_{33}\bar{\zeta}_{52} - \bar{\zeta}_{32}\zeta_{53} + i(\bar{\beta}_2 - \beta_3)\bar{\zeta}_{42}\zeta_{43}]\zeta^*_{51}$$

$$+ [i\bar{\alpha}_2\bar{\zeta}_{32}\zeta_{13} - i\alpha_3\zeta_{33}\bar{\zeta}_{12} - \zeta_{33}D\bar{\zeta}_{32} - \bar{\zeta}_{32}D\zeta_{33} + i\bar{\beta}_2\bar{\zeta}_{32}\zeta_{43}$$

$$- i\beta_3\zeta_{33}\bar{\zeta}_{42}]\zeta^*_{61}\}dy \qquad \text{(B5)}$$

$$h_{52} = \int_0^\infty \{-R[i(\bar{\alpha}_1 - \alpha_3)\bar{\zeta}_{11}\zeta_{13} - \zeta_{33}\bar{\zeta}_{21} - \bar{\zeta}_{31}\zeta_{23} + i\bar{\beta}_1\bar{\zeta}_{11}\zeta_{43} - i\beta_3\zeta_{13}\bar{\zeta}_{41}]\zeta^*_{22}$$

$$- R[i(\bar{\alpha}_1\bar{\zeta}_{41}\zeta_{13} - i\alpha_3\zeta_{43}\bar{\zeta}_{11} - \zeta_{33}\bar{\zeta}_{51} - \bar{\zeta}_{31}\zeta_{53} + i(\bar{\beta}_1 - \beta_3)\bar{\zeta}_{41}\zeta_{43}]\zeta^*_{52}$$

$$+ [i\bar{\alpha}_1\bar{\zeta}_{31}\zeta_{13} - i\alpha_3\zeta_{33}\bar{\zeta}_{11} - \zeta_{33}D\bar{\zeta}_{31} - \bar{\zeta}_{31}D\zeta_{33} + i\bar{\beta}_1\bar{\zeta}_{31}\zeta_{43}$$

$$- i\beta_3\zeta_{33}\bar{\zeta}_{41}]\zeta^*_{62}\}dy \qquad \text{(B6)}$$

$$h_{53} = \int_0^\infty \{-R[-i(\alpha_1 + \alpha_2)\zeta_{11}\zeta_{12} - \zeta_{31}\zeta_{22} - \zeta_{32}\zeta_{21} - i\beta_1\zeta_{11}\zeta_{42} - i\beta_2\zeta_{12}\zeta_{41}]\zeta^*_{23}$$

$$- R[-i\alpha_2\zeta_{42}\zeta_{11} - i\alpha_1\zeta_{41}\zeta_{12} - \zeta_{31}\zeta_{52} - \zeta_{32}\zeta_{51} - i(\beta_2 + \beta_1)\zeta_{42}\zeta_{41}]\zeta^*_{53}$$

$$+ [-i\alpha_2\zeta_{32}\zeta_{11} - i\alpha_1\zeta_{31}\zeta_{12} - \zeta_{31}D\zeta_{32} - \zeta_{32}D\zeta_{31} - i\beta_2\zeta_{32}\zeta_{41}$$

$$- i\beta_1\zeta_{31}\zeta_{42}]\zeta^*_{63}\}dy \qquad \text{(B7)}$$

$$\Gamma_1 = \int^\infty (\alpha_{3i} + \bar{\alpha}_{2i} - \alpha_{1i})\bar{dx} + \int (\beta_{3i} \bar{+} \beta_{2i} \bar{-} \beta_{1i})dz - \bar{\int}(\omega_{3i} + \omega_{2i} - \bar{\omega}_{1i})dt$$

$$+ i\phi \qquad \text{(B8)}$$

$$\Gamma_2 = \int (\alpha_{3i} + \alpha_{1i} - \alpha_{2i})dx + \int (\beta_{3i} + \beta_{1i} - \beta_{2i})dz - \int (\omega_{3i} + \omega_{1i} - \omega_{2i})dt$$

$$+ i\phi \qquad \text{(B9)}$$

$$\Gamma_3 = \int (\alpha_{1i} + \alpha_{2i} - \alpha_{3i})dx + \int (\beta_{1i} + \beta_{2i} - \beta_{3i})dz - \int (\omega_{1i} + \omega_{2i} - \omega_{3i})dt$$

$$- i\phi \tag{B10}$$

where

$$X_n = U - 2i\alpha_n R_,^{-1}$$

$$Z_n = W - 2i\beta_n R_,^{-1}$$

$$\phi = - \int \sigma_x dx_1 - \int \sigma_z dz_1 + \int \sigma_t dt_1,$$

and $(\bar{\ })$ indicates a complex conjugate

Appendix C

$$h_{6n} = \int_0^\infty \{Y_n \zeta_{1n} + R \frac{\partial DU}{\partial x_1} \zeta_{3n}) \zeta^*_{2n} + (Y_n \zeta_{4n} + R \frac{\partial DW}{\partial x} \zeta_{3n}) \zeta^*_{5n_1} - R^{-1} Y_n \zeta_{3n} \zeta^*_{6n}\} dy$$

where

$$Y_n = iR(\alpha_n \frac{\partial U}{\partial x_1} + \beta_n \frac{\partial W}{\partial x_1})$$

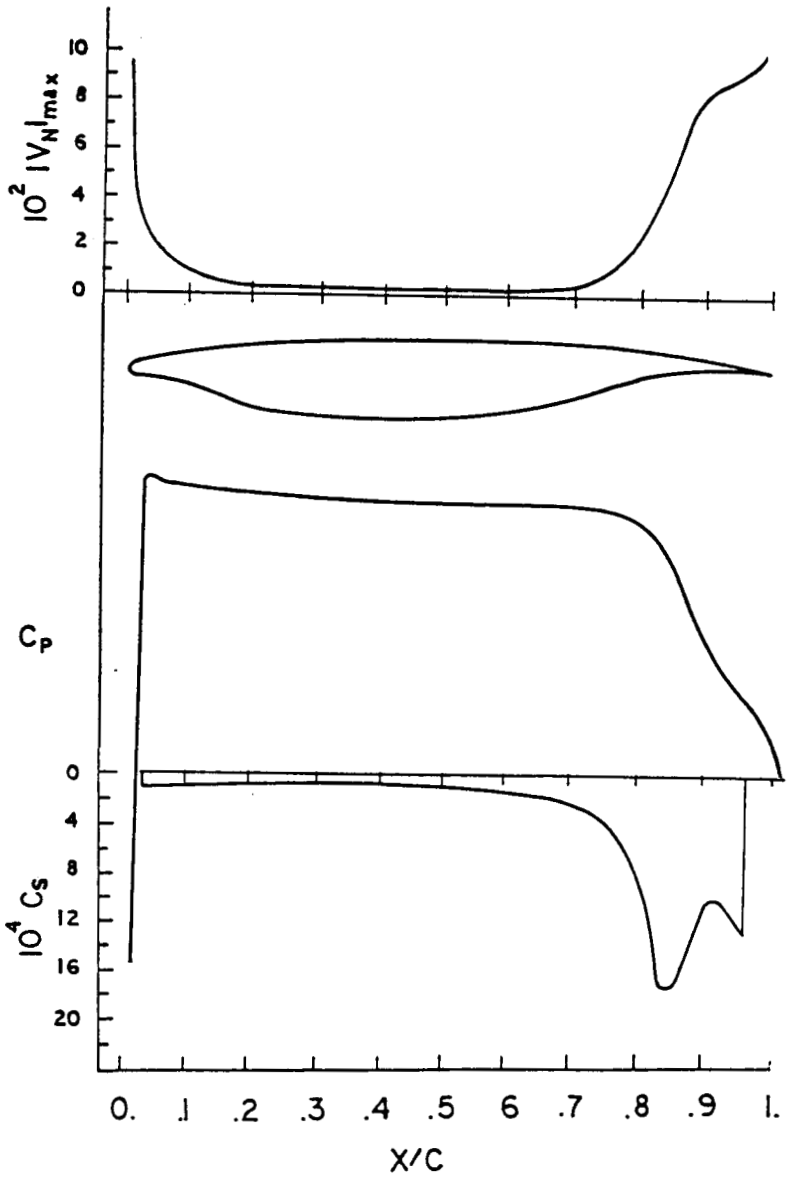

Fig. 1 The distribution on the upper surface of the airfoil of the maximum crossflow component $|V_N|_{max}$, pressure coefficient C_p and suction coefficient C_s along the normal chord.

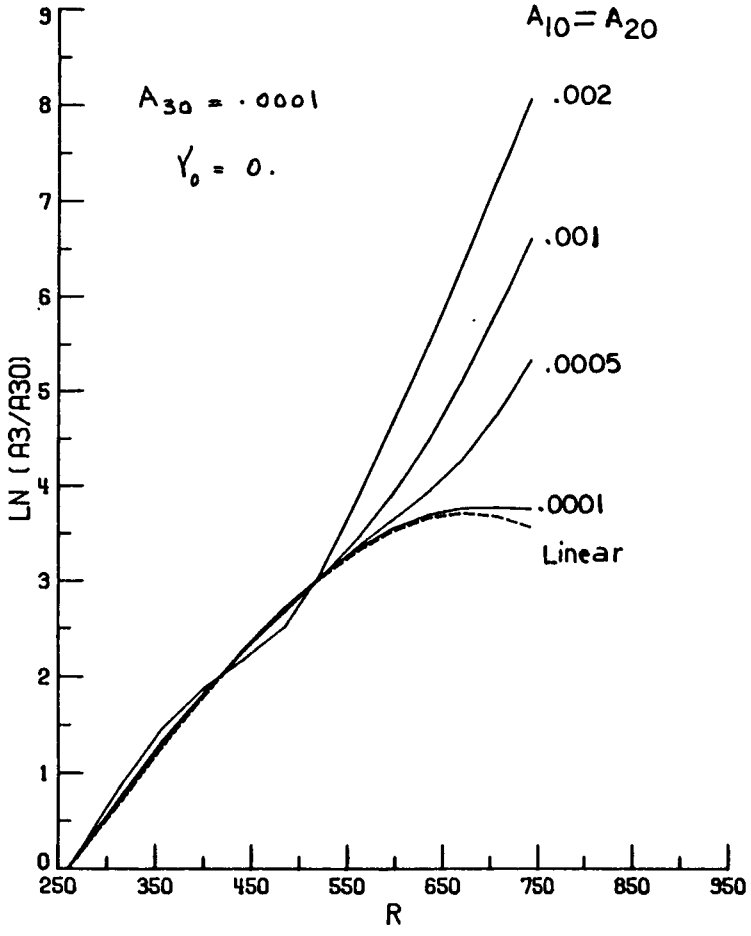

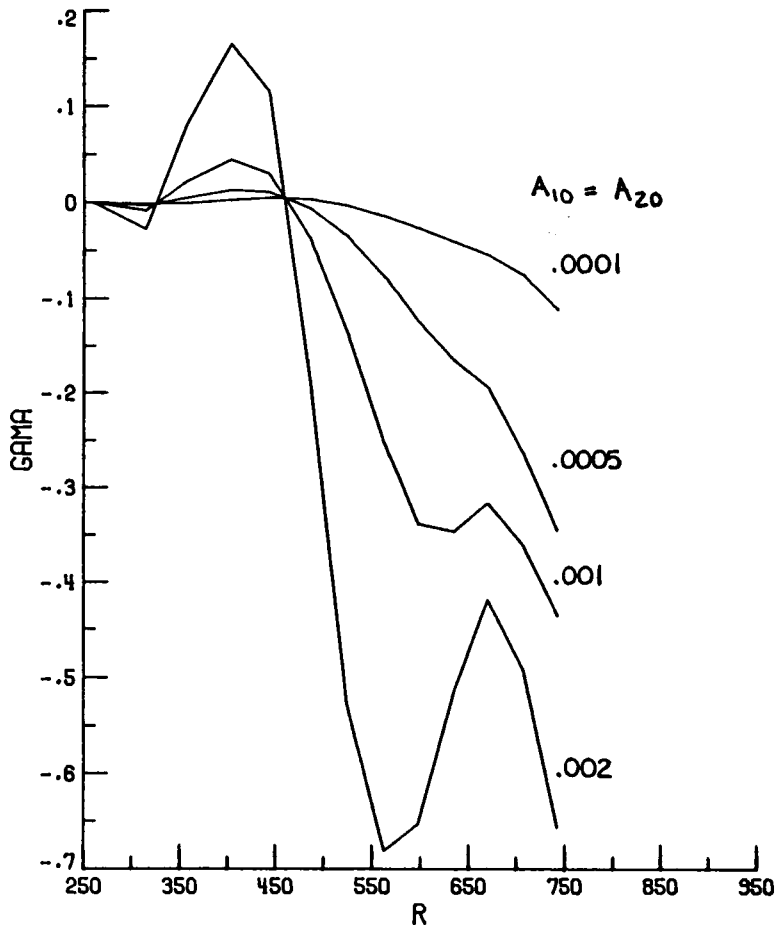

Fig. 2 The modulation of A_3 and γ with R for $A_{30} = 0.0001$, $\gamma_0 = 0$ and various values of A_{10} and A_{20}.

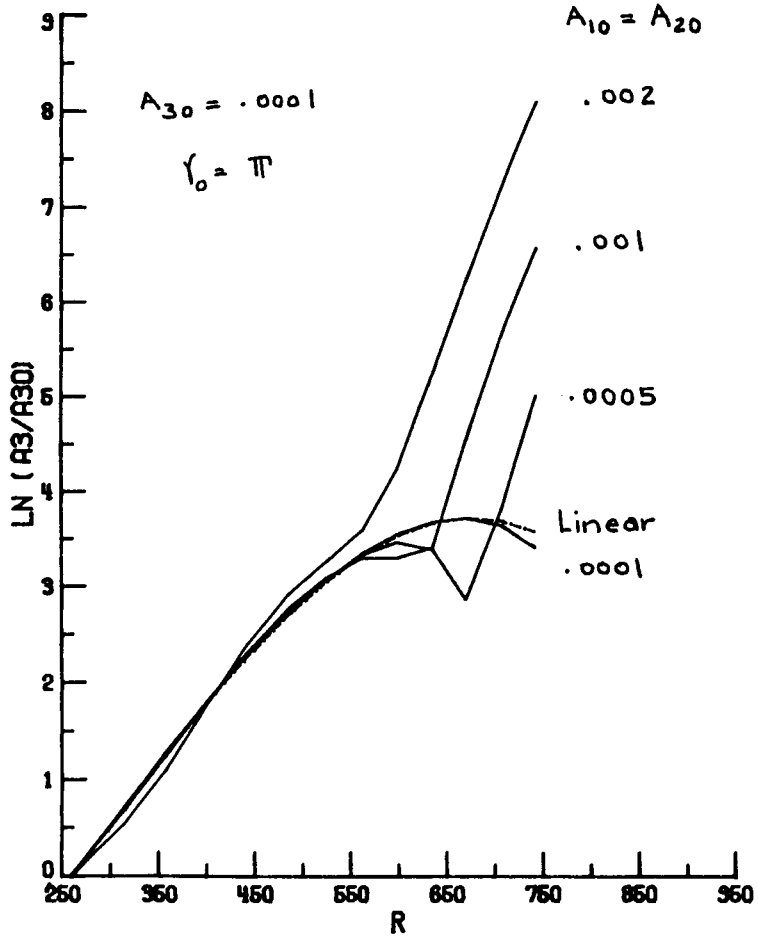

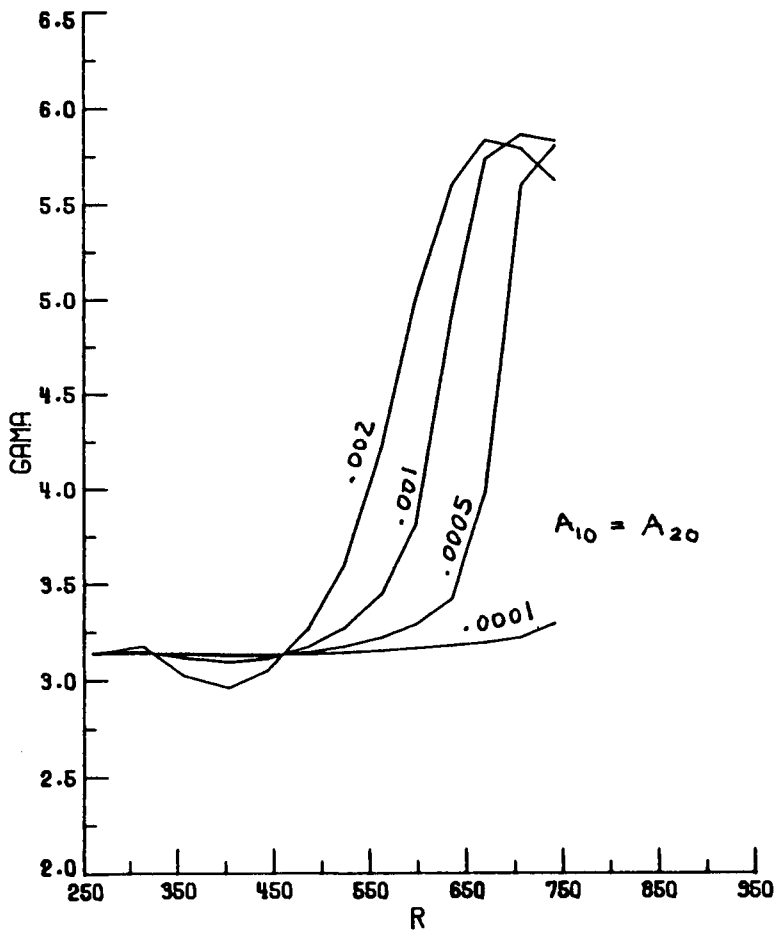

Fig. 3 The modulation of A_3 and γ with R. Same initial conditions as in Fig. 2 but for $\gamma_0 = \pi$.

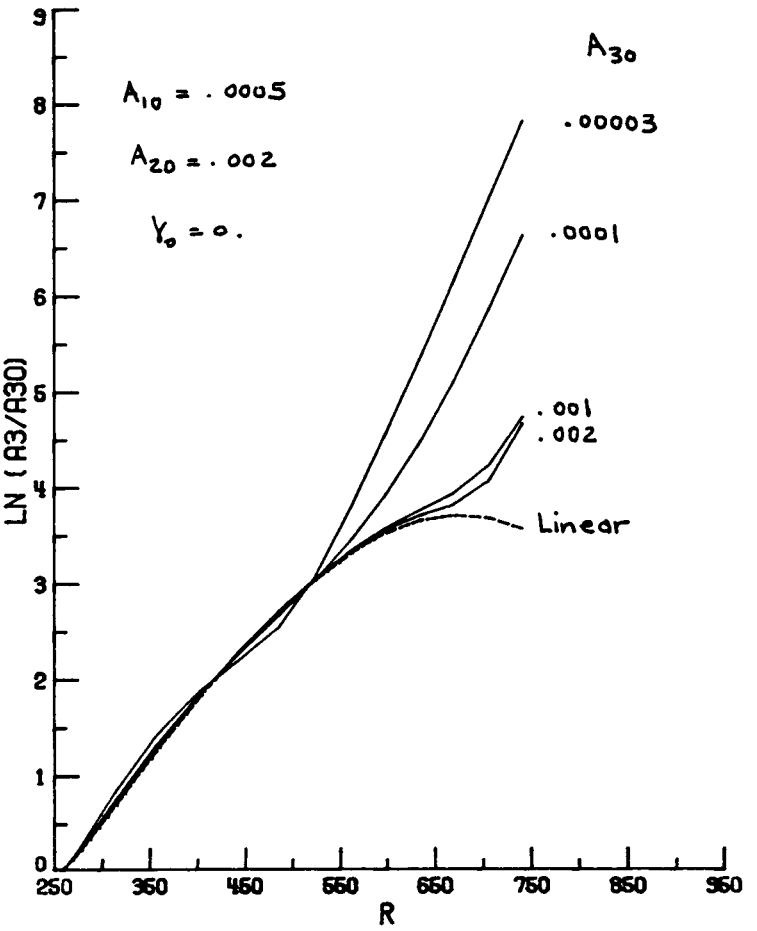

Fig. 4 The modulation of A_3 with R for $A_{10} = 0.0005$, $A_{20} = 0.002$, $\gamma_0 = 0$, and various values of A_{30}

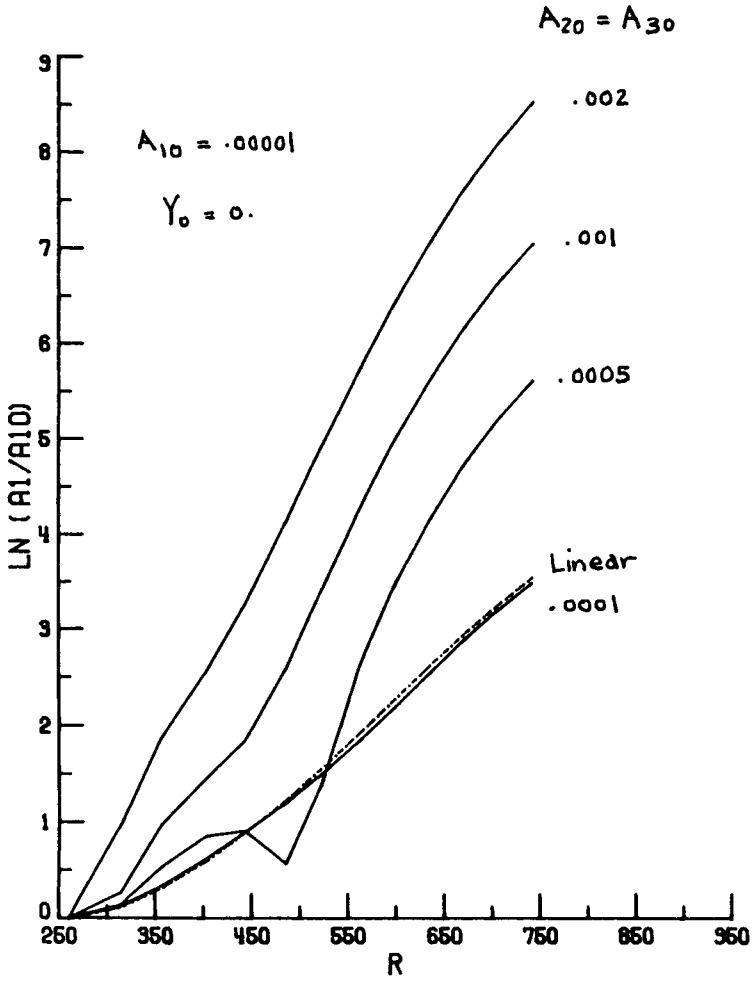

Fig. 5 The modulation of A_1 with R for $A_{10} = 0.00001$, $\gamma_0 = 0$, and various values for A_{20} and A_{30}.

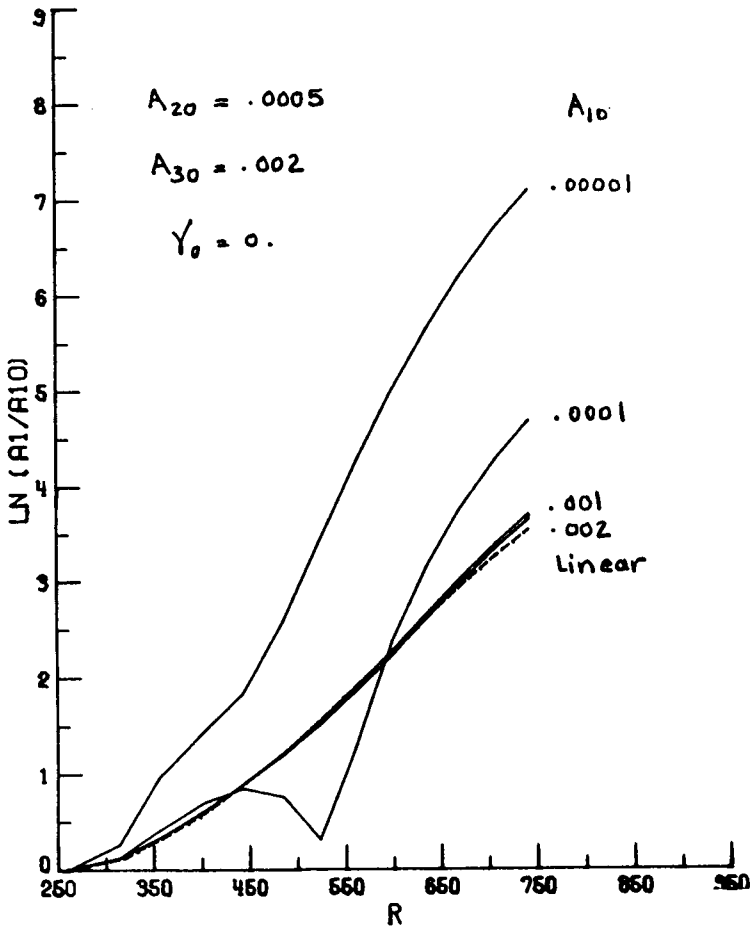

Fig. 6 The modulation of A_1 with R for $A_{20} = 0.0005$, $A_{30} = 0.002$, $\gamma_0 = 0$, and various values of A_{10}

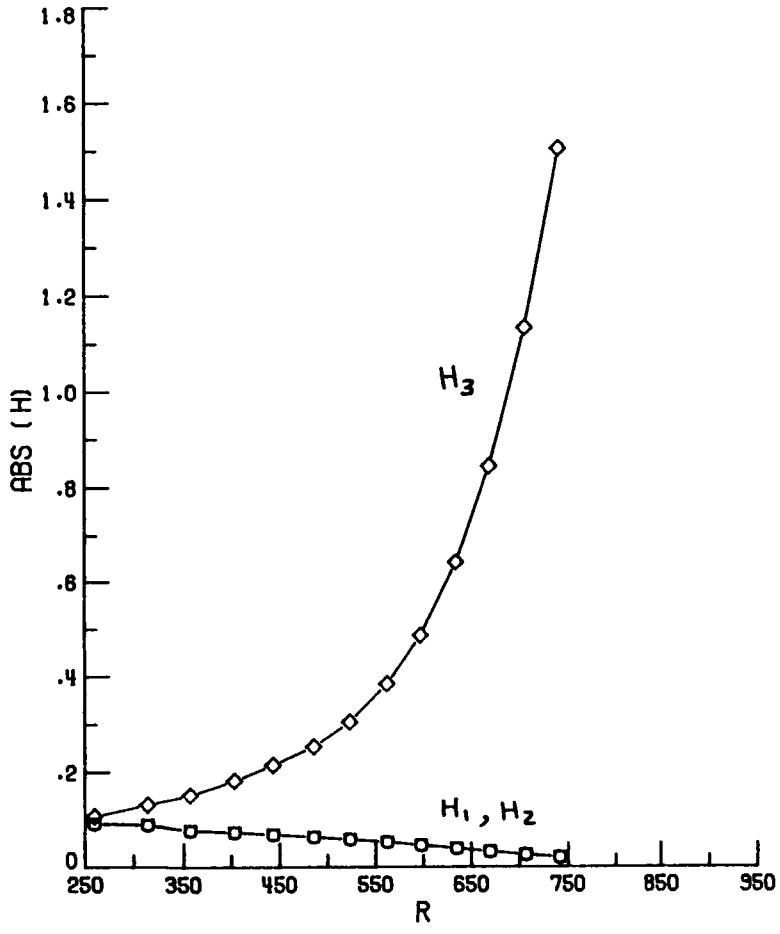

Fig. 7 Variation of the interaction coefficients with R.

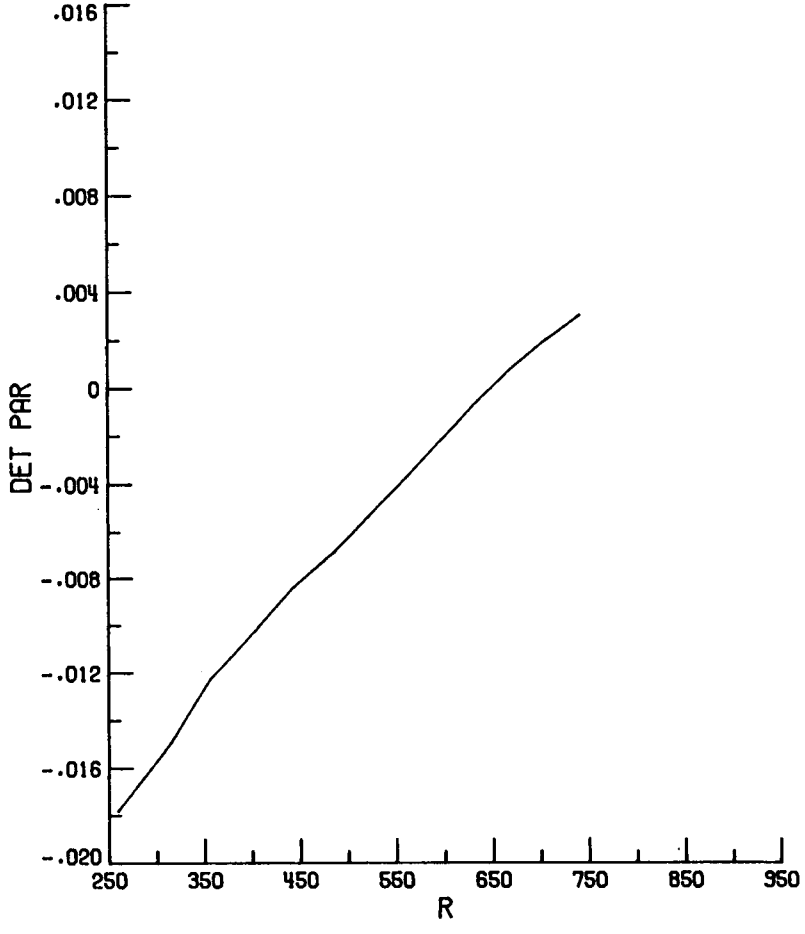

Fig. 8 Variation of the detuning parameter $\varepsilon\sigma_x$ with R.

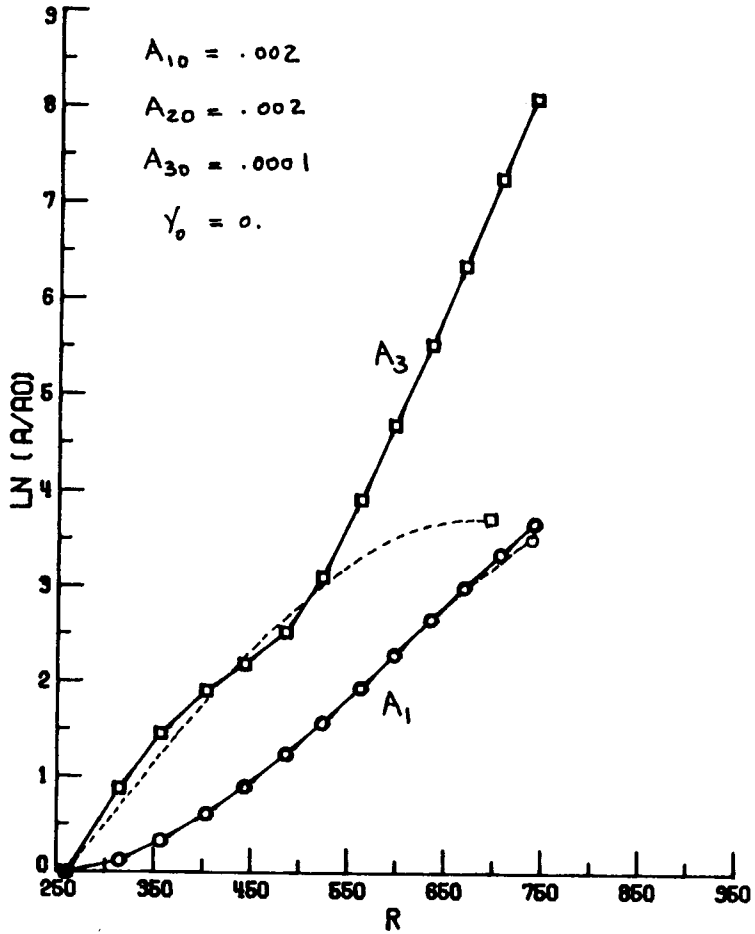

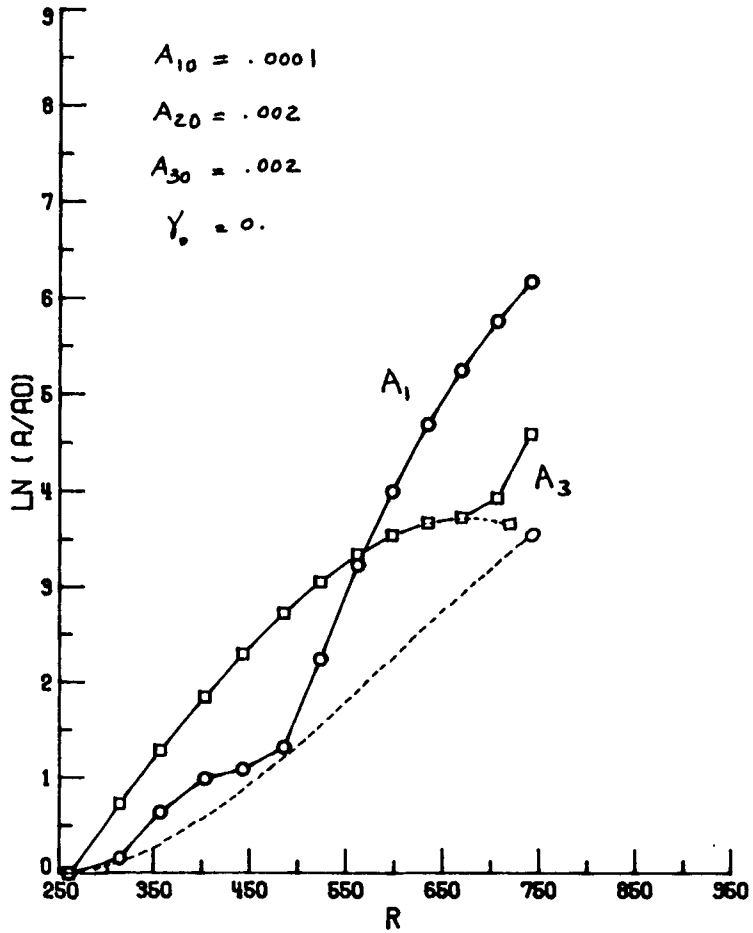

Fig. 9 Amplification of a superharmonic A_3 or Amplification of a subharmonic A_1

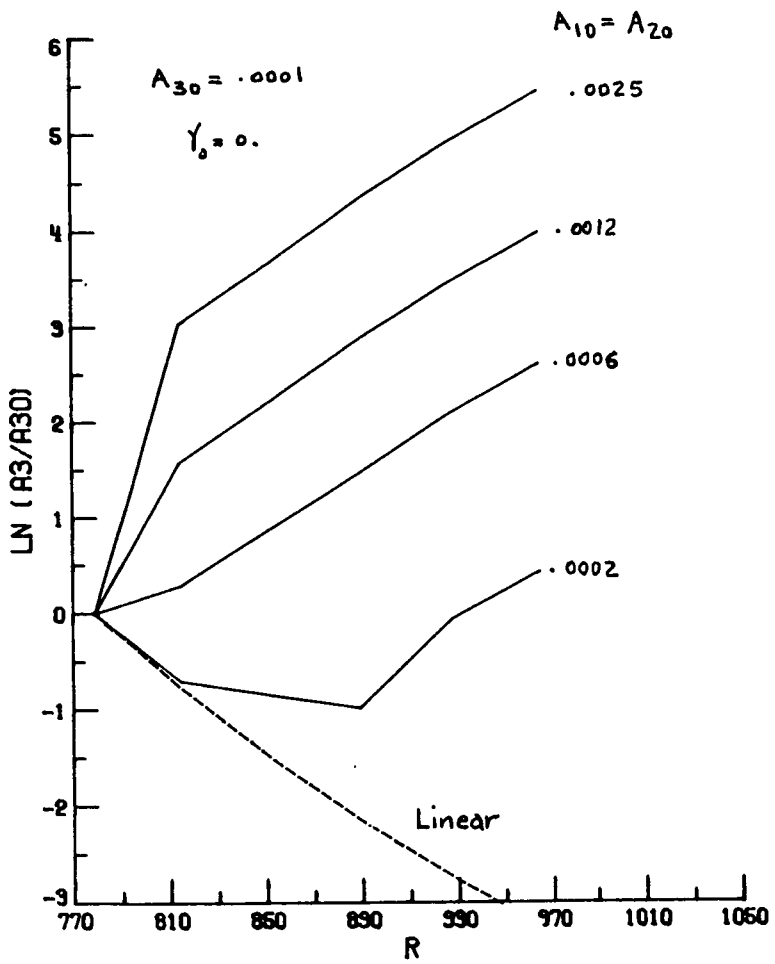

Fig. 10 The modulation of a VV mode with $A_{30} = 0.0001$, $\gamma_0 = 0$ due to resonant interaction with two traveling CF modes of different initial amplitudes $A_{10} = A_{20}$

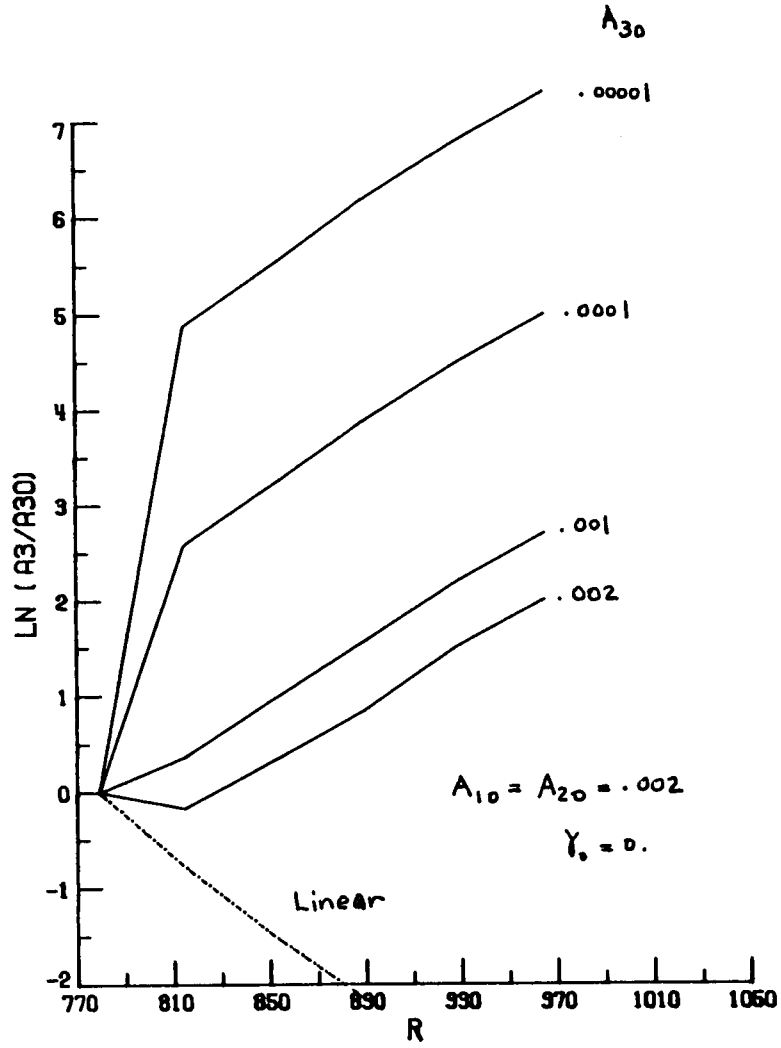

Fig. 11 The modulation of a VV mode with various initial amplitude A_{30} due to resonant interaction with two traveling CF modes A_1, A_2

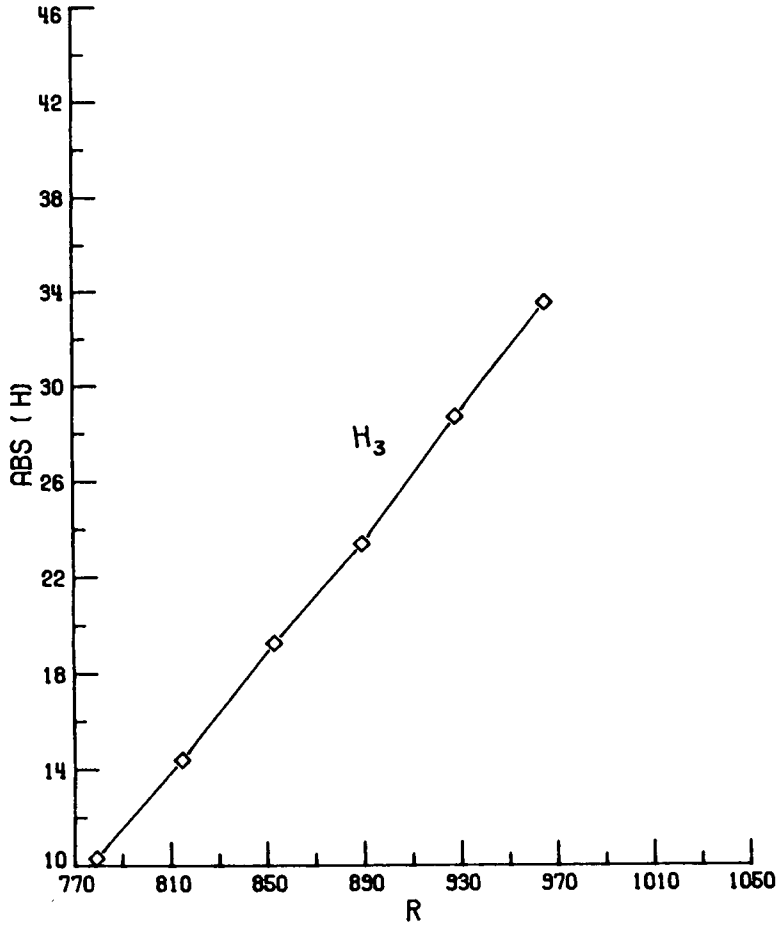

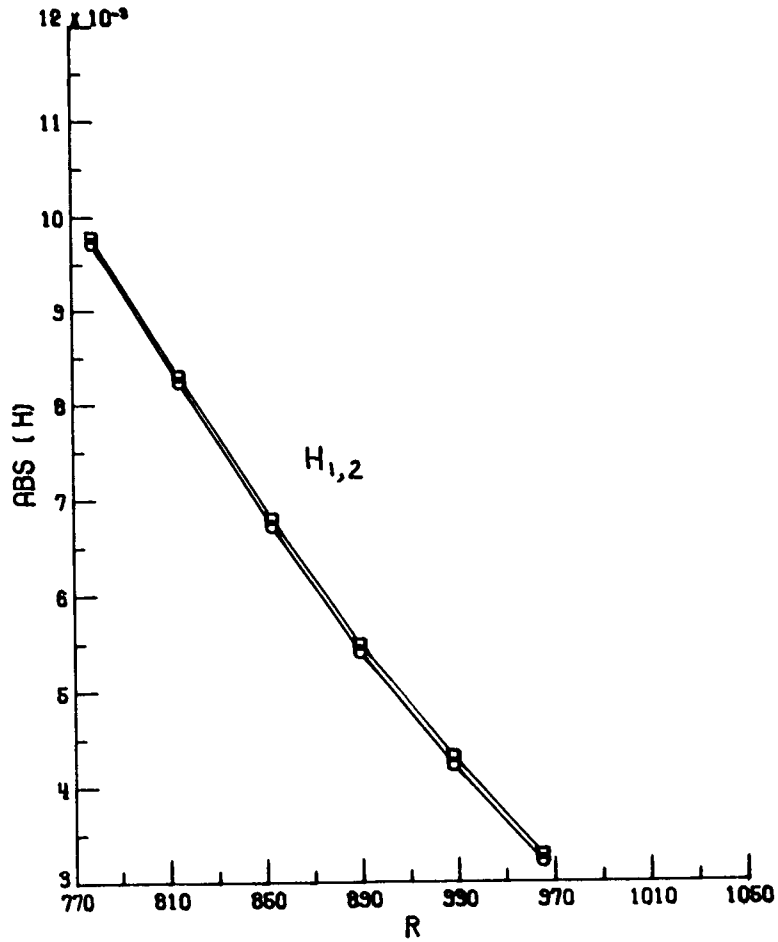

Fig. 12 Variation of the interaction coefficients with R.

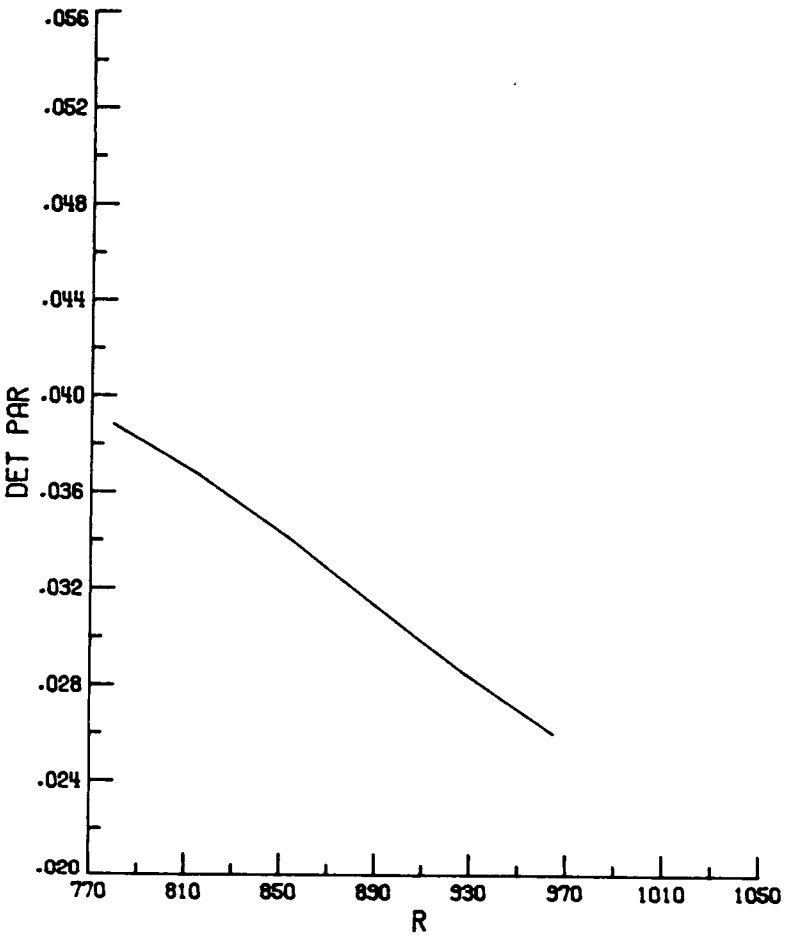

Fig. 13 Variation of the detuning parameter $\varepsilon\sigma_x$ with R.

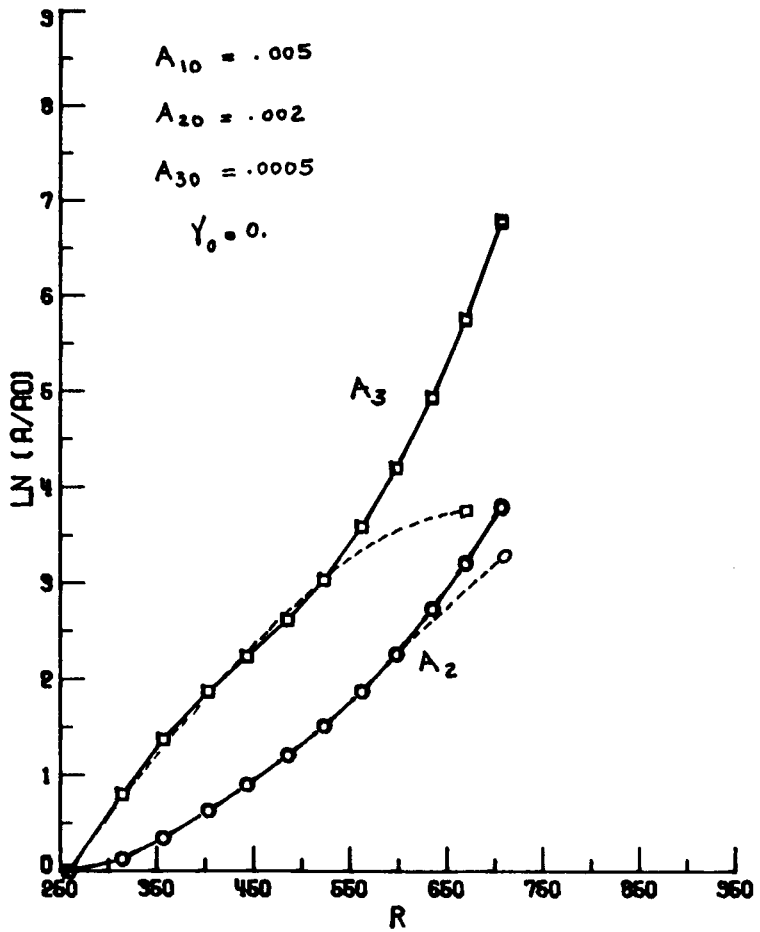

Fig. 14 The modulation of traveling CF modes A_2 and A_3 due to resonant interaction with a stationary CF vortex A_1

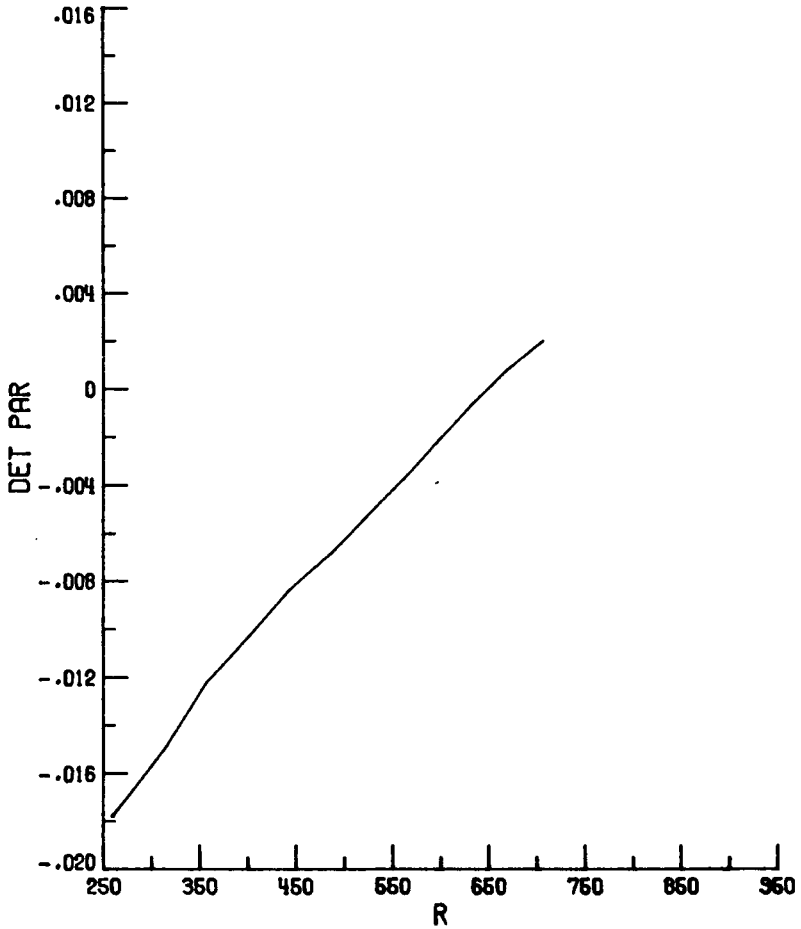

Fig. 15 Variation of the detuning parameter $\epsilon\sigma_x$ with R.

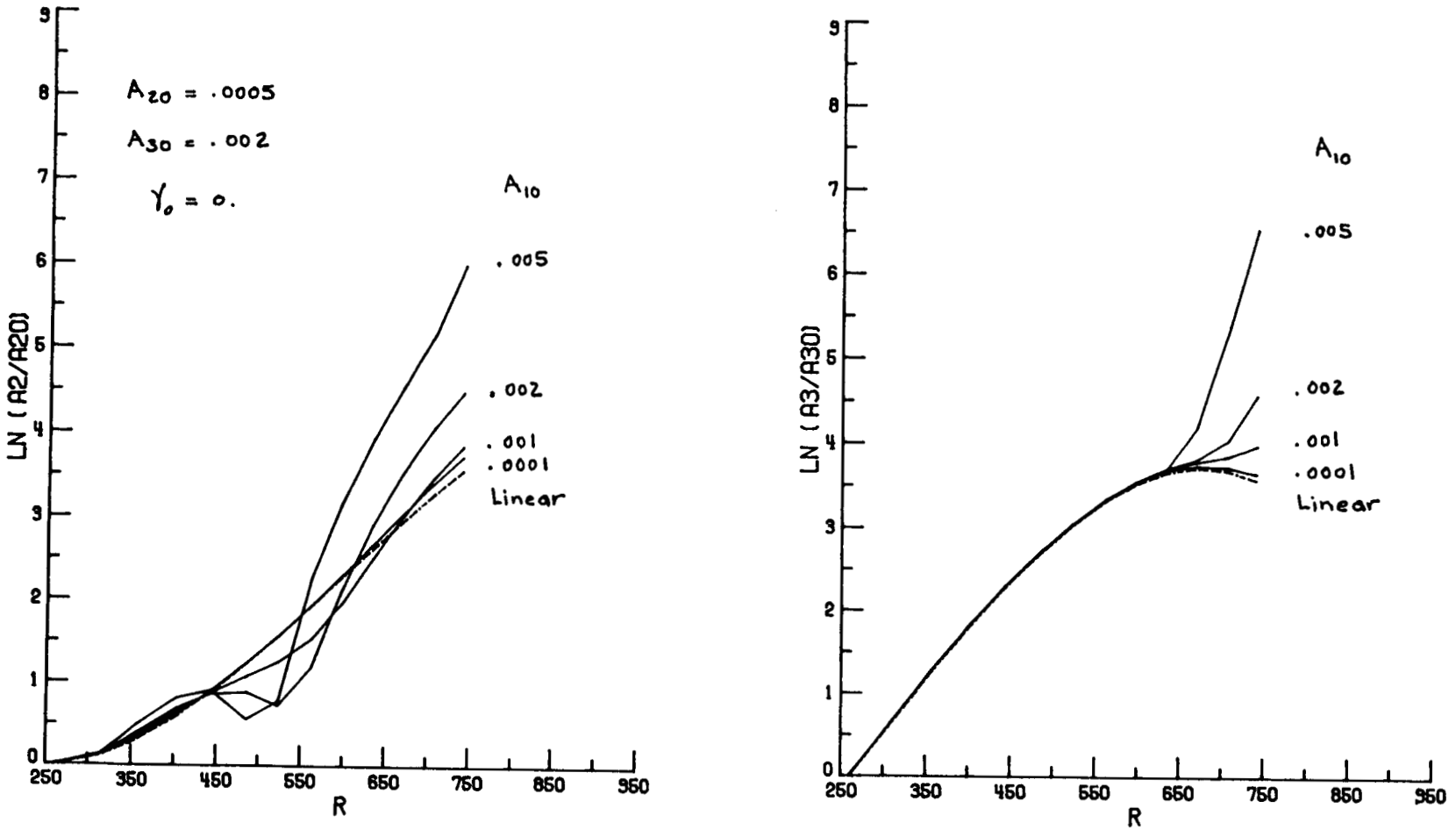

Fig. 16 Effect of the initial amplitude A_{10} of the stationary CF vortex on the modulation of traveling CF modes A_2 and A_3.

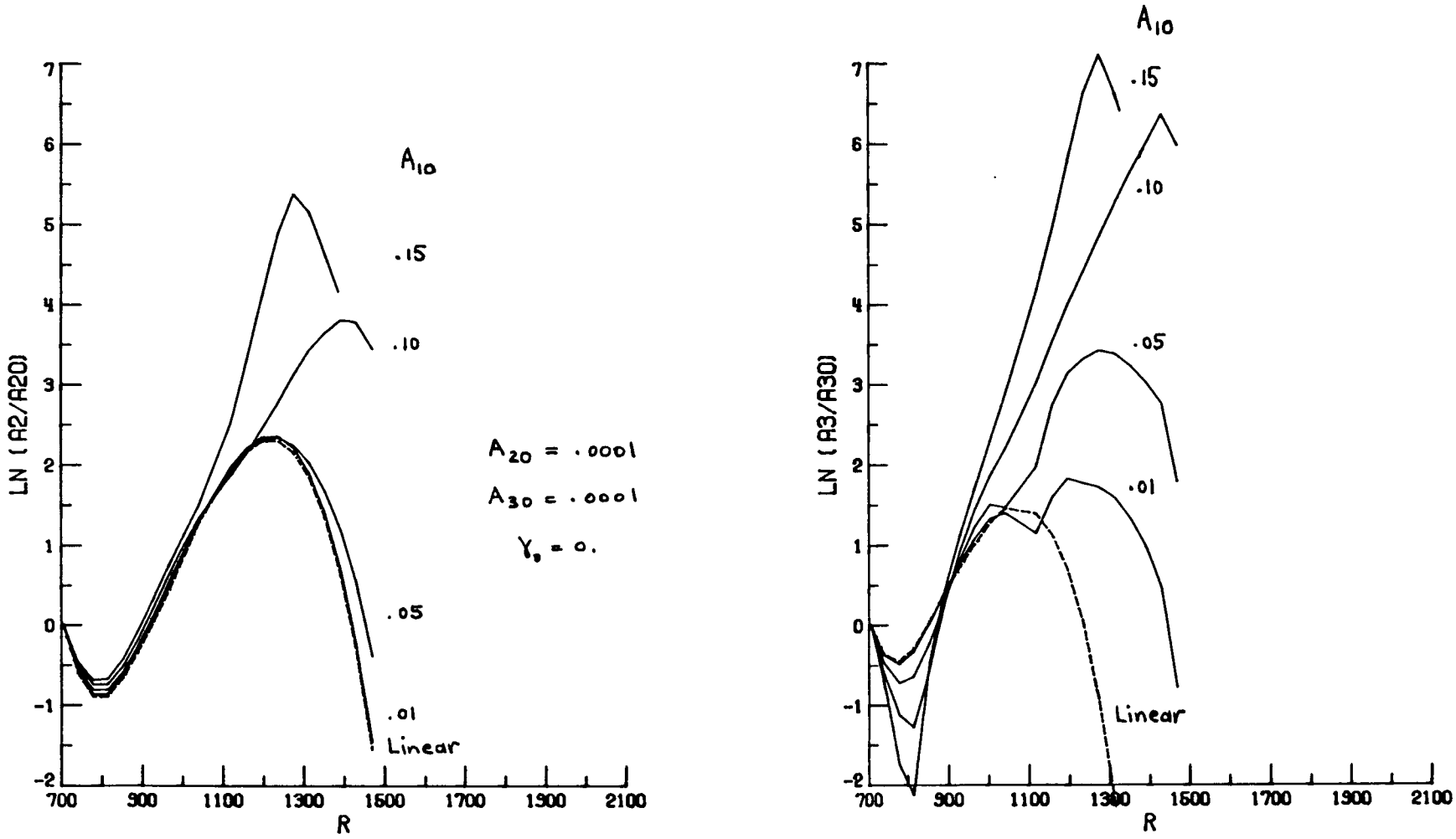

Fig. 17 The modulation of TS modes A_2 and A_3 due to resonant interaction with a stationary CF vortex A_1 with various initial amplitudes

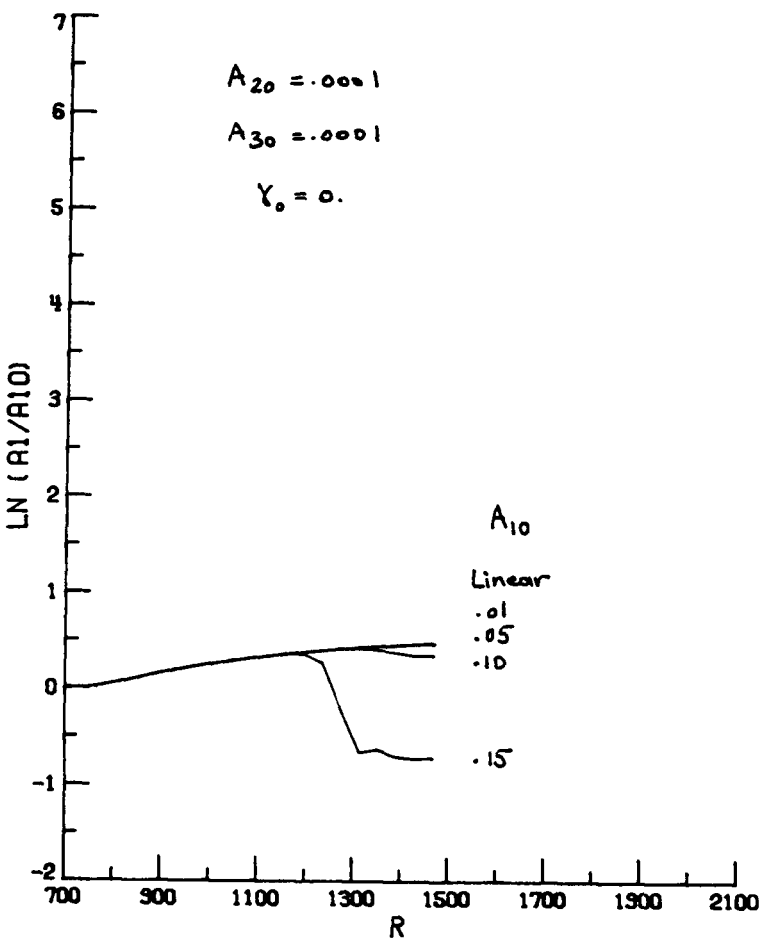

cont. The modulation of the stationary CF vortex A_1 due to resonant interaction with TS modes A_2 and A_3

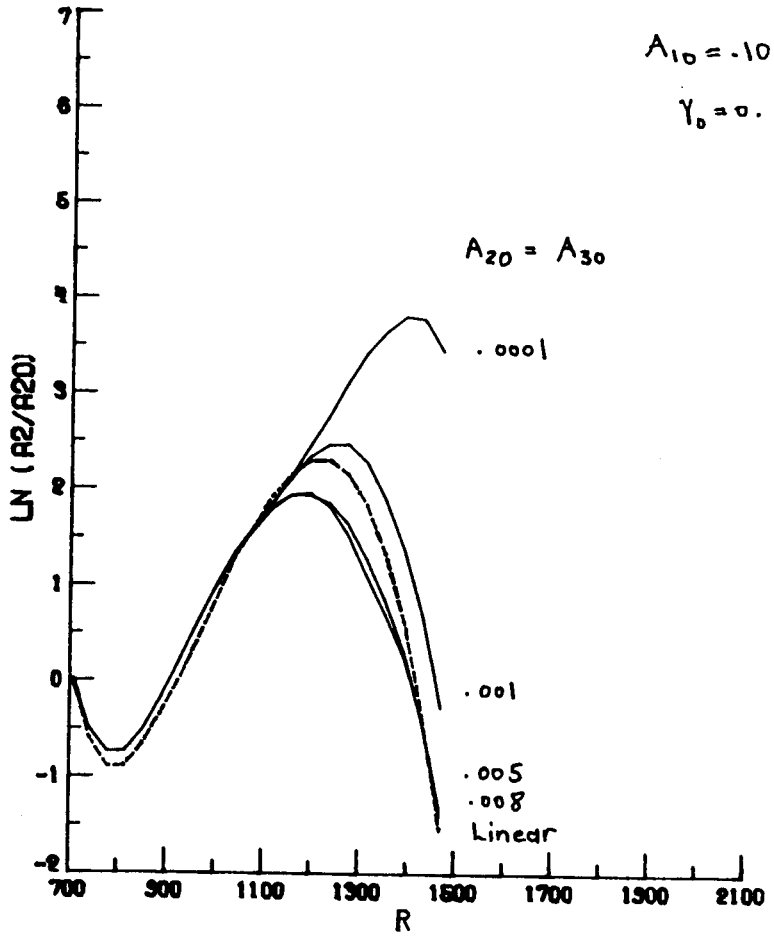

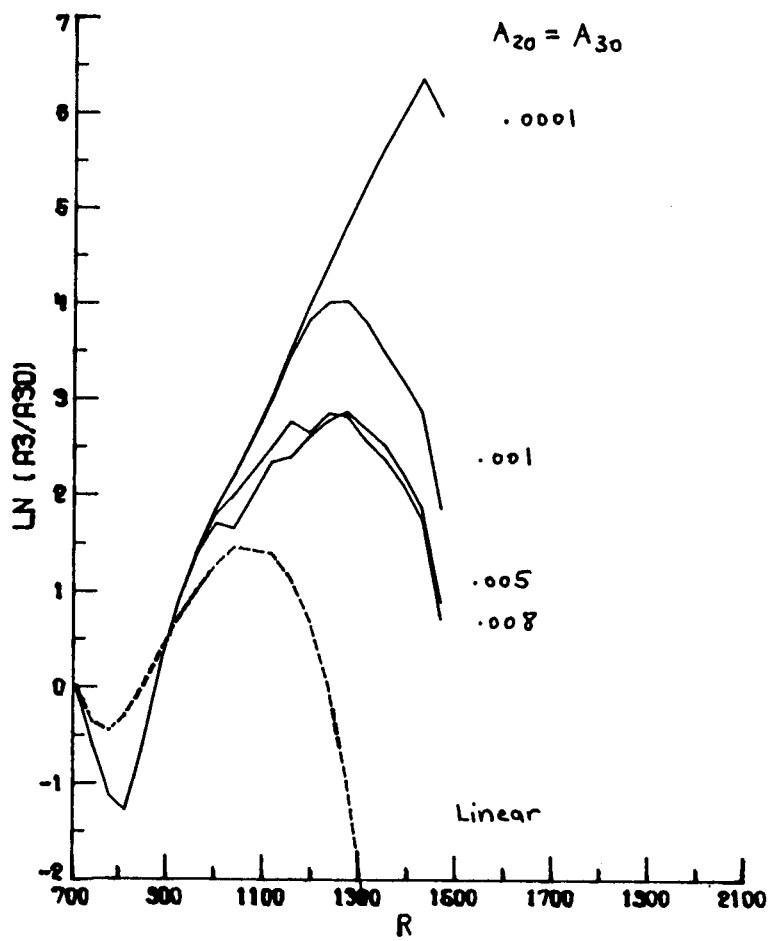

Fig. 18 The modulation of TS modes A_2 and A_3 with various initial amplitudes due to resonant interaction with a stationary CF vortex A_1

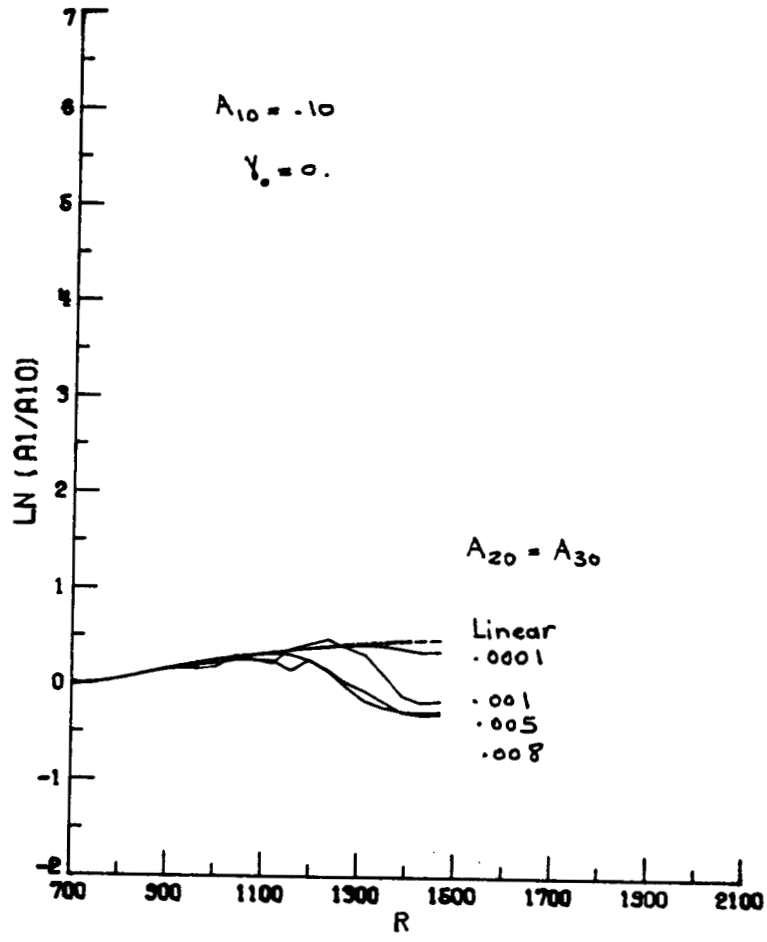

cont. The modulation of the stationary CF vortex A_1 due to resonant interaction with TS modes A_2 and A_3

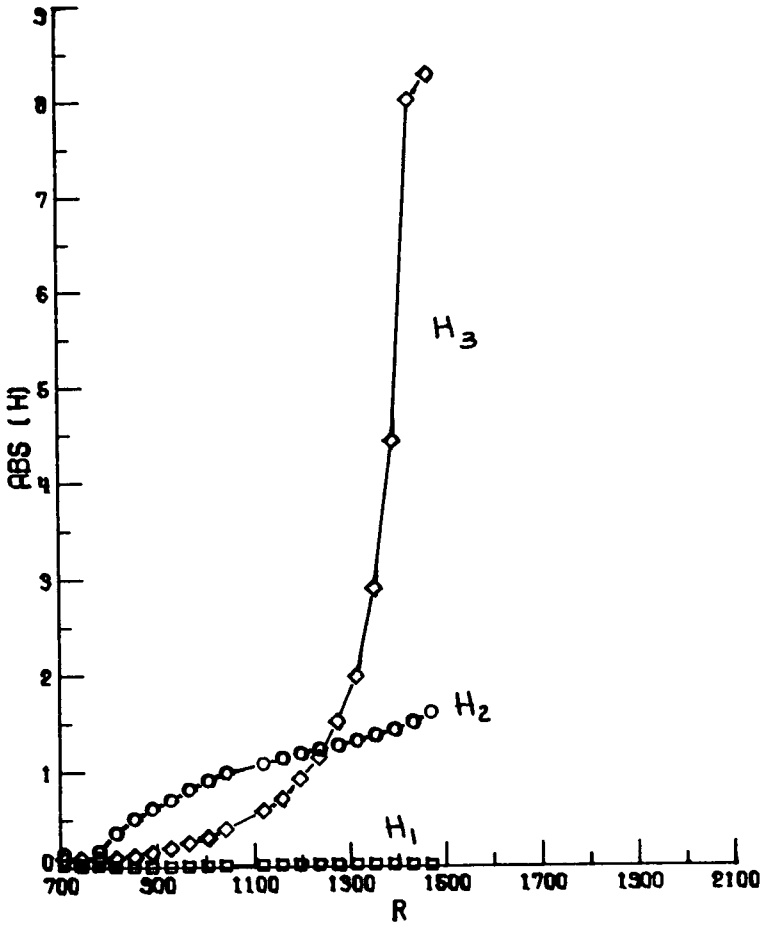

Fig. 19 Variation of the interaction coefficients with R.

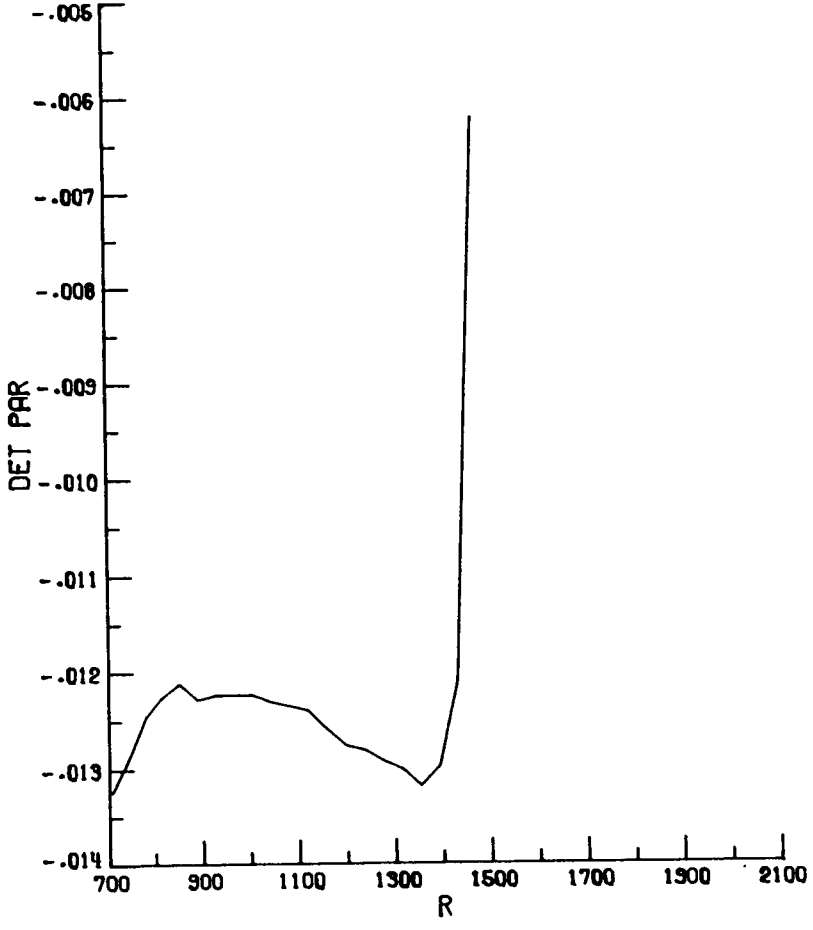

Fig. 20 Variation of the detuning parameter $\epsilon\sigma_x$ with R.

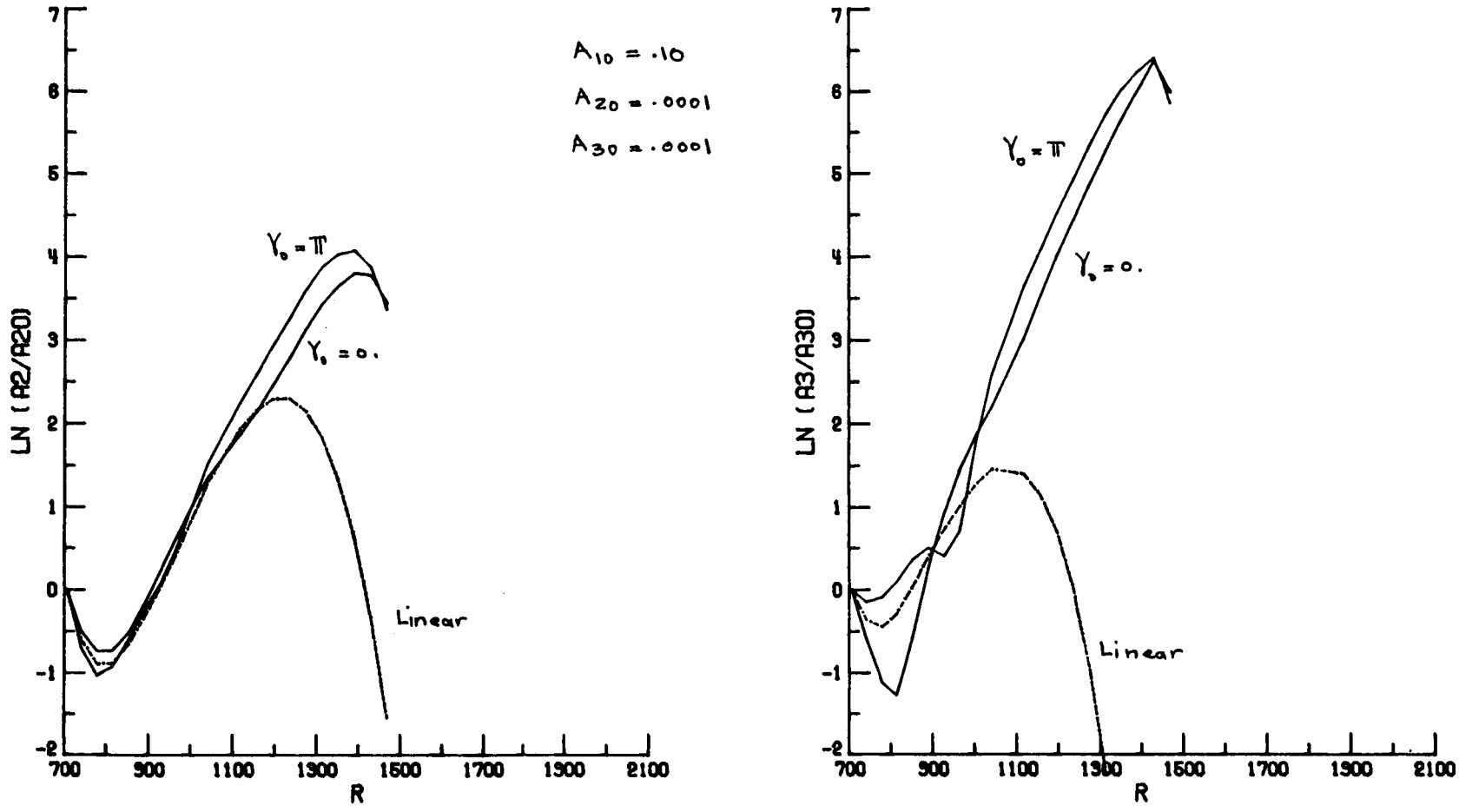

Fig. 21 Effect of γ_0 on the amplification of the TS modes A_2 and A_3 due to resonant interaction with a stationary crossflow vortex A_1.

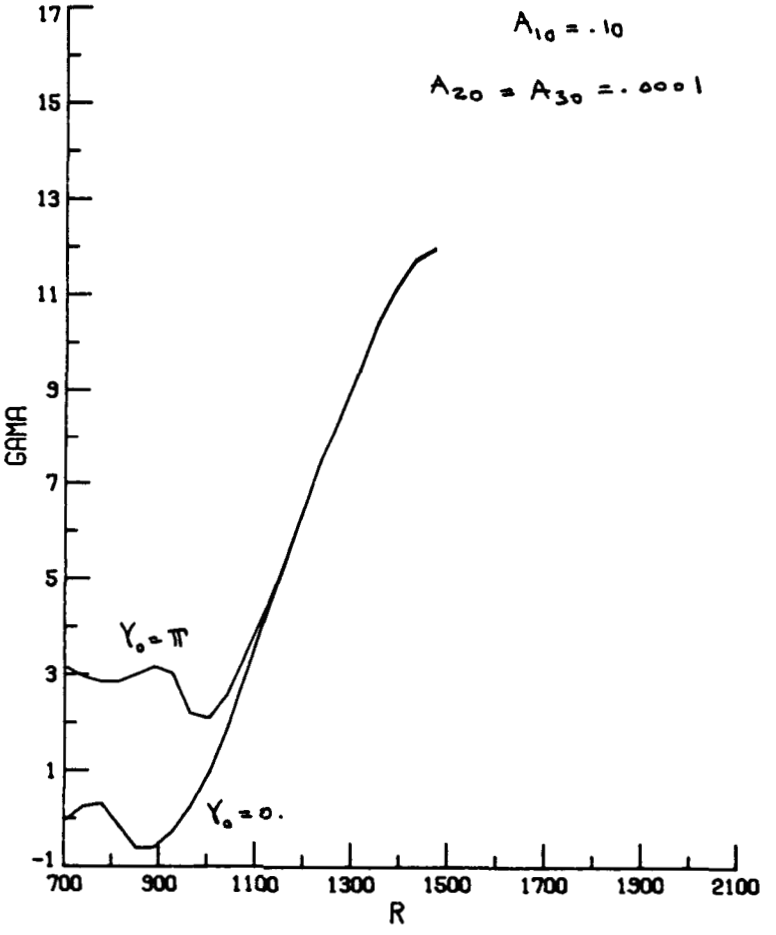

Fig. 22 The modulation of γ with R for the conditions of Fig. 22.

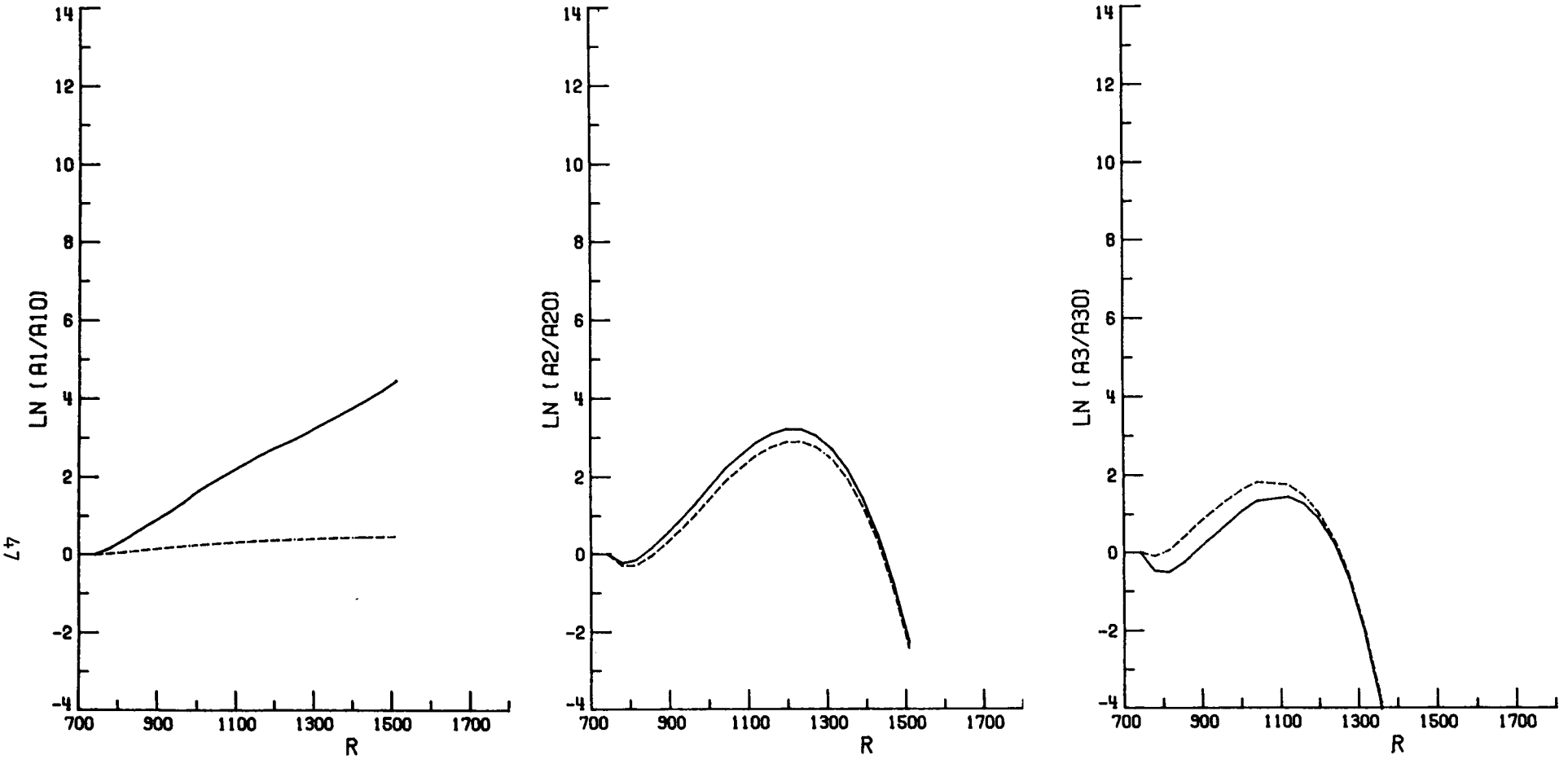

Fig. 23 The linear parallel ----- and linear nonparallel _____ amplitude modulations of a stationary CF mode A_1 and two TS modes A_2 and A_3 given in section 5d.

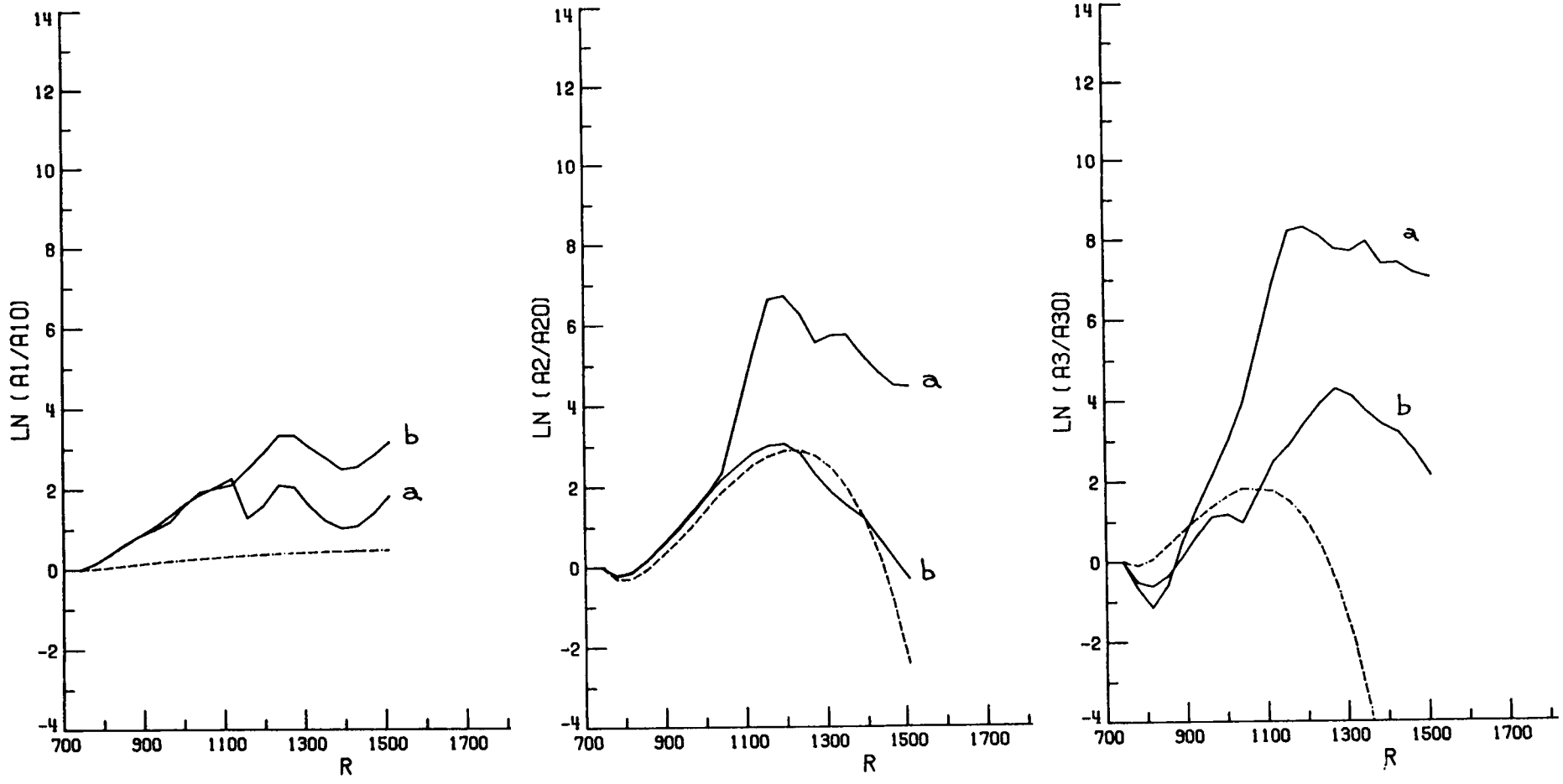

Fig. 24 The nonlinear nonparallel amplitude modulation of a stationary CF mode A_1 and two TS modes A_2 and A_3 given in section 5d for various initial amplitudes of the interacting modes. a) $A_{10} = .05$, $A_{20} = A_{30} = 0.0001$, b) $A_{10} = 0.01$, $A_{20} = A_{30} = 0.005$. Linear parallel -----; nonlinear nonparallel _____.

NASA
National Aeronautics and Space Administration

Report Documentation Page

1. Report No.	2. Government Accession No.	3. Recipient's Catalog No.
NASA CR-4142		

4. Title and Subtitle	5. Report Date
Nonlinear Wave Interactions in Swept Wing Flows	May 1988
	6. Performing Organization Code

7. Author(s)	8. Performing Organization Report No.
Nabil M. El-Hady	
	10. Work Unit No.
	505-60-21-01

9. Performing Organization Name and Address	11. Contract or Grant No.
Old Dominion University Department of Mechanical Engineering and Mechanics Norfolk, VA 23508	NAG1-729
	13. Type of Report and Period Covered
12. Sponsoring Agency Name and Address	Contractor Report
National Aeronautics and Space Administration Langley Research Center Hampton, VA 23665-5225	14. Sponsoring Agency Code

15. Supplementary Notes

Langley Technical Monitor: William D. Harvey

16. Abstract

An analysis is presented that examines the modulation of different instability modes satisfying the triad resonance condition in time and space in a three-dimensional boundary-layer flow. Detuning parameters are used for the wave numbers and the frequencies. The nonparallelism of the mean flow is taken into account in the analysis. At the leading-edge region of an infinite swept wing, different resonant triads are investigated that are comprised of traveling crossflow, stationary crossflow, vertical vorticity, and Tollmien-Schlichting modes. The spatial evolution of the resonating triad components are studied.

17. Key Words (Suggested by Author(s))	18. Distribution Statement
Nonlinear Interaction of Waves in Swept Wing Flows Boundary-Layer Stability Nonlinear Wave Interaction Swept Wing Flows	Unclassified - Unlimited Subject Category 34

19. Security Classif. (of this report)	20. Security Classif. (of this page)	21. No. of pages	22. Price
Unclassified	Unclassified	52	A04

NASA-Langley, 1988